Riluzole treatment modulates KCC2 and EAAT-2 receptor expression and Ca2+ accumulation following ventral root avulsion injury

Krisztián Pajer, Tamás Bellák, Tímea Grósz, Bernát Nógrádi, Roland Patai, József Sinkó, Laurent Vinay, Sylvie Liabeuf, Miklós Erdélyi, Antal Nógrádi

European Journal of Cell Biology 102 (2023) 151311

Contents lists available at ScienceDirect

European Journal of Cell Biology

journal homepage: www.elsevier.com/locate/ejcb

OxLDL sensitizes platelets for increased formation of extracellular vesicles capable of finetuning macrophage gene expression

Katariina Maaninka [a,b,1], Maarit Neuvonen [a,1], Erja Kerkelä [c], Kati Hyvärinen [c], Mari Palviainen [a,b], Masood Kamali-Moghaddam [d], Antonio Federico [e], Dario Greco [e,f], Saara Laitinen [c], Katariina Öörni [g], Pia RM Siljander [a,b,*]

[a] EV group, Molecular and Integrative Biosciences Research Programme, Faculty of Biological and Environmental Sciences, and CURED, Drug Research Program, Faculty of Pharmacy, Division of Pharmaceutical Biosciences, University of Helsinki, Helsinki, Finland
[b] EV Core, Molecular and Integrative Biosciences Research Programme, Faculty of Biological and Environmental Sciences, University of Helsinki, Helsinki, Finland
[c] Finnish Red Cross Blood Service (FRCBS), Helsinki, Finland
[d] Department of Immunology, Genetics and Pathology, Science for Life Laboratory, Uppsala University, Uppsala, Sweden
[e] Finnish Hub for Development and Validation of Integrated Approaches (FHAIVE), Faculty of Medicine and Health Technology, Tampere University, Tampere, Finland
[f] Division of Pharmaceutical Biosciences, Faculty of Pharmacy, University of Helsinki, Helsinki, Finland
[g] Atherosclerosis Research Laboratory, Wihuri Research Institute, Helsinki, Finland

ARTICLE INFO

Key words:
Extracellular vesicle
Platelet
Oxidized low-density lipoprotein
Atherosclerosis
Macrophage
Transcriptome

ABSTRACT

Platelet extracellular vesicles (PEVs) generated upon platelet activation may play a role in inflammatory pathologies such as atherosclerosis. Oxidized low-density lipoprotein (oxLDL), a well-known contributor to atherogenesis, activates platelets and presensitizes them for activation by other agonists. We studied the effect of oxLDL on the secretion, composition, and inflammatory functions of PEVs using contemporary EV analytics. Platelets were activated by co-stimulation with thrombin (T) and collagen (C) ± oxLDL and characterized by high-resolution flow cytometry, nanoparticle tracking analysis, proximity extension assay, western blot, and electron microscopy. The effect of PEVs on macrophage differentiation and functionality was examined by analyzing macrophage surface markers, cytokine secretion, and transcriptome. OxLDL upregulated TC-induced formation of $CD61^+$, P-selectin$^+$ and phosphatidylserine$^+$ PEVs. Blocking the scavenger receptor CD36 significantly suppressed the oxLDL+TC-induced PEV formation, and HDL caused a slight but detectable suppression. The inflammatory protein cargo differed between the PEVs from stimulated and unstimulated platelets. Both oxLDL+TC- and TC-induced PEVs enhanced macrophage HLA-DR and CD86 expression and decreased CD11c expression as well as secretion of several cytokines. Pathways related to cell cycle and regulation of gene expression, and immune system signaling were overrepresented in the differentially expressed genes between TC PEV -treated vs. control macrophages and oxLDL+TC PEV -treated vs. control macrophages, respectively. In conclusion, we speculate that oxLDL and activated platelets contribute to proatherogenic processes by increasing the number of PEVs that provide an adhesive and procoagulant surface, contain inflammatory mediators, and subtly finetune the macrophage gene expression.

Abbreviations: C, collagen; EV, extracellular vesicle; FBS, fetal bovine serum; HDL, high-density lipoprotein; LDL, low-density lipoprotein; LOD, limit of detection; MFI, median fluorescence intensity; MØ, macrophage; NPX, normalized protein expression; oxLDL, oxidized low-density lipoprotein; oxTC MØ, macrophages treated with oxLDL + thrombin and collagen-induced platelet-derived EVs; PEA, proximity extension assay; PEV, platelet-derived extracellular vesicle; PS, phosphatidylserine; SEC, size exclusion chromatography; T, thrombin; TC MØ, macrophages treated with thrombin and collagen-induced platelet-derived EVs; TBARS, thiobarbituric acid reactive substances; UC, ultracentrifugation.

* Corresponding author.
E-mail addresses: katariina.maaninka@helsinki.fi (K. Maaninka), neuvonen.maarit@gmail.com (M. Neuvonen), erja.kerkela@veripalvelu.fi (E. Kerkelä), kati.hyvarinen@veripalvelu.fi (K. Hyvärinen), mari.palviainen@helsinki.fi (M. Palviainen), masood.kamali@igp.uu.se (M. Kamali-Moghaddam), antonio.federico@tuni.fi (A. Federico), dario.greco@tuni.fi (D. Greco), saara.laitinen@veripalvelu.fi (S. Laitinen), kati.oorni@wri.fi (K. Öörni), pia.siljander@helsinki.fi (P.R. Siljander).
[1] Equal contribution, alphabetical order.

https://doi.org/10.1016/j.ejcb.2023.151311
Received 26 August 2022; Received in revised form 10 March 2023; Accepted 14 March 2023
Available online 15 March 2023

1. Introduction

Atherosclerosis is a slowly progressing disease characterized by lipid accumulation and unresolved inflammation. Over time, the continuous lipid accumulation and series of cellular proinflammatory events lead to the development of inflamed fatty deposits called atherosclerotic plaques. Rupture of plaques leads to thrombotic episodes manifested as myocardial infarction or stroke contributing to high mortality and morbidity. A key risk factor for atherosclerotic cardiovascular disease is dyslipidemia, particularly an increased level of low-density lipoprotein (LDL) cholesterol (Ference et al., 2017). In addition, an increased concentration of oxidatively modified LDL (oxLDL) in circulation is associated with cardiovascular diseases (Trpkovic et al., 2015).

A defining feature of atherogenesis is the entry of blood monocytes into the arterial intima, and their differentiation into macrophages (MØ), which actively internalize the retained lipoproteins giving rise to lipid-laden foam cells (Boren et al., 2020). The accumulation of foam cells promotes plaque formation, and infiltrating MØs also contribute to lesion formation by maintaining a proinflammatory microenvironment. Decreased ability of the plaque MØs to migrate hampers the resolution of inflammation and drives the progression of more advanced plaques (Barrett, 2020). In the absence of efficient efferocytosis, apoptotic MØs ultimately contribute to the necrotic core formation in the plaques promoting the progression of the lesions into complicated, rupture-prone plaques (Bäck et al., 2019). Thus, MØs and their differentiation play a decisive role at all stages of the atherosclerotic lesion progression, yet, not all the mechanistic factors behind their involvement have been elucidated.

Similarly, platelets represent an important cell type contributing to atherogenesis both in its early and more advanced stages (Massberg et al., 2002; Panigrahi et al., 2013). Platelets interact either directly or indirectly with several cell types, and of these interactions, those with monocytes are critical during atherogenesis. Platelets promote the uptake of oxLDL by monocytes and MØs, inhibit monocyte apoptosis, and induce monocyte migration and recruitment to atherosclerotic plaques (Scheuerer et al., 2000; Badrnya et al., 2014; Barrett et al., 2019). Platelets also regulate monocyte functions by modulating their activation, differentiation, and polarization. For example, platelet chemokine C-X-C motif chemokine 4 (CXCL4) has been shown to promote MØ differentiation by inducing a unique phenotype, M4, whose prevalence in human atherosclerotic lesions has been associated with plaque instability (Erbel et al., 2015). More recently, platelets were shown to skew MØ differentiation towards an inflammatory phenotype with impaired phagocytosis, sustaining unresolved inflammation and plaque growth (Barrett et al., 2019).

A distinguishing feature of platelets is their agility to generate extracellular vesicles (EVs) (Gasecka et al., 2019; Puhm et al., 2021). Platelet-derived EV (PEV) release can be triggered by the activation of platelets with various physiological stimuli (Aatonen et al., 2012; Boilard et al., 2015; Milioli et al., 2015), the most potent of which is the co-stimulation via multiple thrombin (T) and collagen (C) receptors (Aatonen et al., 2014). Increased circulating numbers of PEVs have been reported in cardiovascular high-risk patients and patients with atherosclerosis compared to healthy individuals (Tan et al., 2005; Zhang et al., 2014; Suades et al., 2015) supporting the emerging evidence that also PEVs may contribute to atherogenesis (Zaldivia et al., 2017; Konkoth et al., 2021; Badimon et al., 2022; Coly and Boulanger, 2022). Although, the mechanisms of PEVs' proatherogenic functions are not fully elucidated, it was recently shown that PEVs had a natural homing ability to atherosclerotic plaques in ApoE$^{-/-}$ mice (Ma et al., 2021). PEVs contain a dynamic molecular cargo including nucleic acids [messenger RNAs (mRNAs), micro RNAs (miRNAs), and long non-coding RNAs (lncRNAs)], lipid mediators, biogenic amines, and numerous proteins such as cytokines, chemokines, and growth factors (Aatonen et al., 2012; Gasecka et al., 2019; Valkonen et al., 2019; Suades et al., 2022). Also, the membrane composition of PEVs may be significant for their functionality as it harbors many molecular determinants of cell adhesion, activation, and coagulation. These include various glycoproteins such as the integrin complex CD41/CD61, CD62P (P-selectin), and CD40 ligand (CD40L) (Aatonen et al., 2012; Gasecka et al., 2019). Another essential feature for the function of PEVs is the membrane lipid composition, which comprises e.g. procoagulant phospholipids such as phosphatidylserine (PS), and other phospholipids that can be processed into bioactive lipid mediators via arachidonic acid for crosstalk with leukocytes (Boilard, 2018).

In patients with familial hypercholesterolemia, a genetic disorder characterized by high plasma LDL cholesterol levels, increased leukocyte EV and PEV numbers predicted future cardiovascular events and reflected ongoing innate immune cell and platelet activation (Suades et al., 2019). An increased number of PEVs in the circulation is considered to manifest platelet activation, and dyslipidemia, especially the elevated plasma cholesterol levels, contributes to platelet hyperactivity (Carvalho et al., 1974; Shastri et al., 1980; Harmon et al., 1986). Also the interaction of platelets with oxLDL has been shown to enhance platelet reactivity (Davi et al., 1998; Colas et al., 2011; Biswas et al., 2017; Berger et al., 2020) and to aggravate atherogenesis and thrombosis (Podrez et al., 2007; Yang et al., 2017; Berger et al., 2020). *In vitro,* oxLDL has been shown to preactivate platelets rendering them susceptible to activation by other agonists (Weidtmann et al., 1995; Korporaal et al., 2005; Nergiz-Unal et al., 2011). Platelets express members of scavenger receptors and Toll-like receptors (TLRs) (Saboor et al., 2013), both of which are known to recognize and interact with oxLDL (Levitan et al., 2010). The best-known receptor mediating the platelet-activating effect of oxLDL is class B scavenger receptor CD36 (Korporaal et al., 2007; Magwenzi et al., 2015; Berger et al., 2020). Via CD36, oxLDL turns on an intracellular signaling cascade in platelets with downstream effects such as the exposure of P-selectin and PS, and the activation of CD41/CD61 (Nergiz-Unal et al., 2011; Yang et al., 2018). Reversely, high-density lipoprotein (HDL), known for its anti-inflammatory and antiatherogenic properties, has been shown to attenuate platelet activation (Ardlie et al., 1989), thus putatively diminishing the effects of activation initiated by oxLDL (Takahashi et al., 1996). Although oxLDL is known to contribute to platelet activation, the role of oxLDL in PEV formation is controversial with only two studies reporting contradicting data (Wang et al., 2012; Nielsen et al., 2015). We reinvestigated this question by utilizing contemporary sensitive EV analytics and state-of-the-art isolated lipoproteins.

2. Materials and methods

2.1. LDL and HDL isolation and LDL oxidation

Human LDL (d=1.019–1.050 g/ml) was isolated from the plasma of healthy donors (Finnish Red Cross Blood Service [FRCBS]) by sequential ultracentrifugation (UC) in the presence of 3 mM EDTA as previously described (Havel et al., 1955; Radding and Steinberg, 1960). Total human HDL fraction (d=1.063–1.210) was also isolated by sequential UC as previously described (Havel et al., 1955) from serum samples of healthy volunteers with informed consent according to the ethical guidelines of the Finnish Institute of Health and Welfare (THL, Finland). The amount of lipoproteins was determined in terms of their protein content by the BCA Protein Assay Kit (Thermo Scientific). For oxidation, LDL was first diluted to a concentration of 2 mg/ml in Dulbecco's modified phosphate-buffered saline (DPBS) and dialyzed 3 × 24 h against DPBS to remove EDTA, after which LDL was incubated with 10 μM $CuSO_4$/mg LDL for 4 h at 37 °C. Oxidation was stopped with the addition of EDTA at a final concentration of 1 mM. The degree of oxidation was determined by measuring the amount of thiobarbituric acid reactive substances (TBARS) (Hessler et al., 1983).

2.2. Platelet isolation and activation

Platelets were isolated from freshly prepared platelet concentrates obtained from FRCBS (Helsinki). Each concentrate was a pool of 4 donors and contained on average 238 × 10^9 platelets. The residual white blood cell count was on average 0.02 × 10^6 (as measured by FRCBS quality control). Before isolation, 100 ng/ml prostaglandin E1 (Sigma) and 1:10 acid citrate dextrose (39 mM citric acid [Sigma], 75 mM sodium citrate [Sigma], 135 mM [D]-glucose [Sigma], pH 4.5) was added to the platelets, followed by centrifugation at 900 x g for 15 min at room temperature (RT) without brake. The platelets were then resuspended in calcium-free Tyrode-Hepes Buffer (THB; 137 mM NaCl, 0.3 mM NaH2PO4, 3.5 mM Hepes, 5.5 mM [D]-glucose, pH 7.35), and isolated with 10 ml Sepharose CL-2B (GE Healthcare) SEC columns as a void volume (Siljander and Lassila, 1999). Platelet concentration was determined with haematology analyzer (Beckman Coulter T-540, Beckman Coulter Inc) and adjusted to 2.5 × 10^8/ml with THB supplemented with 1 mM $MgCl_2$, 2 mM $CaCl_2$, and 3 mM KCl. In a typical experiment, the isolated platelets were preincubated ± 100 μg/ml oxLDL, a concentration commonly used for in vitro experiments (Hulten et al., 2005; Rubic and Lorenz, 2006; Lara-Guzman et al., 2018) for 2.5 h at 37 °C, and then stimulated by 2 μg/ml collagen (HORM, Takeda) and 0.2 U/ml thrombin (Enzyme Research Laboratories Ltd.) for an additional 30 min at 37 °C for maximal PEV release (Aatonen et al., 2014). Unstimulated platelets incubated in THB supplemented with 1 mM $MgCl_2$, 2 mM $CaCl_2$, and 3 mM KCl for 3 h at 37 °C were used as a control. Additionally, platelets were preincubated with oxLDL in the presence and absence of HDL for 2.5 h followed by stimulation by TC for an additional 30 min. In these experiments, HDL 50 μg/ml at the time of oxLDL addition and 100 μg/ml 30 min prior to oxLDL addition were added to platelets. To block platelet CD36 and TLR4, platelets were preincubated for 30 min at 37 °C with 10 μg/ml mouse anti-human CD36 (clone FA6–152, Stemcell Technologies), 10 μg/ml mouse anti-human TLR4 (clone HTA125, eBioscience), or with a combination of these two, or with their respective isotype-matched negative controls (10 μg/ml mouse IgG1 and 10 μg/ml mouse IgG2a [clone P3.6.2.8.1 and eBM2a, eBioscience], respectively), after which oxLDL (at 100 μg/ml) was added for 2.5 h at 37 °C, and finally the platelets were stimulated for an additional 30 min at 37 °C by TC. Platelets preincubated with DPBS instead of anti-CD36 and anti-TLR4 followed by the addition of oxLDL and TC as described above, were used as a positive control. After stimulation, platelets were sedimented at 5000 x g for 5 min and immediately at 11,000 x g for 1 min both at RT, after which the supernatant was collected and centrifuged at 2500 x g for 25 min at RT to ensure complete removal of platelet remnants, which was verified with the hematology analyzer. The platelet-free supernatants were collected and immediately used for further analyses or PEV isolation.

2.3. PEV isolation

The platelet-free supernatant was centrifuged at 110,000 x g for 2 h at 4 °C with Optima LE-80 K ultracentrifuge with 50.2 Ti rotor, k factor 143.3 (Beckman Coulter), after which the pelleted PEVs were resuspended in 500 μl of DPBS filtered with a 0.1 μm filter unit (Millex VV, Millipore), and centrifuged again at 110,000 x g for 1.5 h at 4 °C with Optima MAX-XP ultracentrifuge with TLA-55 rotor, k factor 81.3 (Beckman Coulter). Finally, the isolated PEVs were resuspended in DPBS filtered with a 0.1 μm filter unit and stored at − 80 °C for further analysis.

2.4. Flow cytometry of PEVs

Twenty-five μl of platelet-free supernatant (at least in two technical replicates) was incubated with 4 μl of phycoerythrin (PE)-conjugated mouse anti-human CD61 (clone VI-PL2, BD Biosciences), 3.125 μl of fluorescein isothiocyanate (FITC)-conjugated bovine lactadherin (Haematologic Technologies), or 3.75 μl PE-conjugated mouse anti-human CD62P (clone AK-4, BD Bioscience) for 1 h at RT in the dark. Protein aggregates were removed from lactadherin-FITC by centrifugation at 19,000 x g for 5 min at RT prior to use. Isotype-matched controls at the same concentration as the specific antibody were used as negative controls. After incubation, the samples were diluted 1:15 with 10 mM Hepes − 140 mM NaCl, pH 7.2 (NH buffer) filtered with a 0.1 μm filter unit. All samples were analyzed on an Apogee A50-Micro (Apogee Flow Systems Ltd. UK) at a flow rate of 1.5 μl/min and keeping the count rate < 4000 events/s to avoid swarm detection. The flow rate was calibrated using Apogee bead mix (Apogee Flow Systems Ltd.) by measuring the concentration of 110 nm FITC-labeled polystyrene beads. Each sample was measured for at least 90 s, triggering on 405 nm side scatter (SSC). The data analyses were performed with FlowJo™ (v10.7.1; FlowJo, LLC). A Rosetta Calibration system (Exometry, Amsterdam, The Netherlands) was used to calibrate light scatter signals and to determine the diameter gates for the used flow cytometer (Van Der Pol et al., 2018). Based on the light scatter calibration, a detectable EV diameter gate of 200–1000 nm was set, in which the lower limit was set to exclude noise and the upper limit was to exclude platelets. Next fluorescent gates were determined for every marker using unlabeled PEVs and isotype controls. Positive events ($^+$) were defined as events with fluorescent signal exceeding the gate. The representative scatter plots and gating strategy are presented in Supplementary Fig. A.1. The data are presented as concentrations i.e. the number of detected events corrected for the total sample dilution, flow rate, and measurement time. The buffer used for the EV dilution as well as free antibody/lactadherin in buffer were used as additional controls according to MIFlowCyt-EV guidelines (Welsh et al., 2020).

2.5. Analysis of particle concentration and protein content

Particle enumeration was performed by nanoparticle tracking analysis (NTA) using Nanosight LM14 (Malvern Instruments Ltd, Malvern, UK) equipped with a blue laser (405 nm, 70 mW) and an sCMOS camera (Hamamatsu Photonics, Hamamatsu, Japan). The isolated PEVs were diluted in 0.1 μm filtered DPBS to obtain 40–100 particles/frame, and 5 × 30 s videos were recorded with the camera level 13. The data were analyzed using NTA 3.0 software (Amesbury, UK) with the detection threshold 7 and the screen gain at 10. To measure PEV protein content, PEVs were first treated with 0.5% Triton-X-100, after which the protein concentration was determined with the DC assay (Bio-Rad) according to the manufacturer's instructions.

2.6. Transmission electron microscopy

Negative staining of the whole mounted EV samples was performed as previously described (Puhka et al., 2017). Briefly, EVs were loaded on 200 mesh pioloform carbon-coated glow discharged copper grids, fixed with 2% PFA, stained with 2% neutral uranyl acetate, embedded in methyl cellulose uranyl acetate mixture (1.8/0.4%), and viewed with Tecnai 12 (FEI Company, Eindhoven, The Netherland) at 80 kV.

2.7. Western blot

Selected proteins enriched in PEVs, namely CD41, CD63, CD9, TSG101, as well as a negative control, calnexin, were analyzed from the PEV isolates by western blotting according to the MISEV guidelines (Thery et al., 2018). Furthermore, apoB-100, the major protein constituent of LDL, was analyzed from the PEV isolates to confirm that oxLDL was depleted during the PEV isolation. For SDS-PAGE, platelets and PEVs were lysed with Laemmli sample buffer either with (for CD41, TSG101, calnexin, ApoB) or without (for CD9 and CD63) 1% β-mercaptoethanol. Ten micrograms of total platelet protein or alternatively 2 × 10^9 PEVs were loaded per lane of Mini-Protean TGX 4–20% precast gels (Bio-Rad) and run at a constant voltage of 180, after which the

proteins were electroblotted to PVDF membranes. The membranes were blocked for 1 h at RT with 1% milk in Tris-buffered saline containing 0.1% Tween-20 (TBST), after which the membranes were incubated overnight at 4 °C with the following primary antibodies: 1:1000 mouse anti-human apoB (Medix Biochemica, Espoo, Finland), 1:5000 mouse anti-human CD41 (clone sz22, Becaman Coulter), 1:1000 mouse anti-human CD9 (clone C-4, Santa Cruz Biotechnologies), 1:250 mouse anti-human TSG101 (clone 51, BD Biosciences), 1:1000 mouse anti-human CD63 (clone H5C6, BD Pharmingen), and 1:1000 rabbit anti-human calnexin (clone C5C9, Cell Signaling Technologies). The excess primary antibodies were washed 4 × 10 min with TBST, after which the membranes were incubated either with 1:3000 HRP-conjugated sheep anti-mouse IgG (GE Healthcare) or with 1:50 000 HRP-conjugated goat anti-rabbit IgG (Jackson Laboratories) for 1 h at RT. Finally, the membranes were washed 4 × 10 min with TBST and the protein bands were detected with ECL substrate (Clarity Western ECL, Bio-Rad) according to the manufacturer's instructions.

2.8. Proximity extension assay

Protein cargo of the PEVs was analyzed by the Proximity Extension Assay (PEA) technology (Assarsson et al., 2014; Larsson et al., 2015; Larssen et al., 2017) using Olink® Inflammation panel (Olink Proteomics, Uppsala, Sweden; Table 1 in Supplementary Material). For that purpose, the PEV samples were run at a concentration of 90 μg/ml. Data were analyzed by Olink NPX (Normalized Protein eXpression) Manager 0.0.104.0 and expressed as NPX values calculated from Ct values. Data normalization (against extension control and interplate control) was performed to minimize both intra-and inter-assay variation. Values below the limit of detection (LOD) were replaced by LOD/2 for statistical analysis.

2.9. Macrophage polarization assay

MØs were differentiated in vitro from isolated human peripheral blood mononuclear cells (PBMCs) as previously described (Hyvärinen et al., 2018) with minor modifications. Briefly, PBMCs were isolated from buffy coats of healthy anonymous blood donors (FRCBS, Helsinki, Finland) by density gradient centrifugation using Ficoll-Paque™ Plus (GE Healthcare Life Sciences). The isolated PBMCs were washed three times with DPBS and incubated at a concentration of 2×10^6 PBMC/ml in Costar 24-well plates (Corning Incorporated) in RPMI 1640 (Gibco) at 37 °C, 5% CO_2 for 2 h, after which the non-adherent cells were removed by DPBS wash. The adherent cells were cultured for 6 days in MØ growing medium (RPMI 1640 supplemented with GlutaMAX™ Supplement [Gibco], 10% FBS [Sigma-Aldrich], and 50 ng/ml granulocyte-macrophage colony-stimulating factor [GM-CSF]) in the absence or presence of 5×10^9/ml oxLDL+TC-induced and TC-induced PEVs. The MØ growing medium ± PEVs was renewed on day 3. On day 6, the cells were activated with 50 ng/ml interferon (IFN)-γ and 10 ng/ml lipopolysaccharide (LPS) in the MØ growing medium in the absence or presence of the PEVs. In each case, three batches of PEVs, each batch representing a different biological replicate consisting of PEVs from four donors, were pooled in a 1:1:1 no. ratio. On day 9, the conditioned media were collected, centrifuged at 300 x g for 15 min, and stored at − 80 °C until further analysis. The MØs were lysed in RLT plus buffer (Qiagen) containing 1% β-mercaptoethanol for RNA isolation or alternatively detached with MØ Detachment Solution DFX (PromoCell) for flow cytometric analysis.

Table 1
Concentration (pg/ml) of cytokines/chemokines secreted by macrophages upon treatment with PEVs.

Analyte	Control MØ		oxTC MØ		TC MØ	
	Median	IQR	Median	IQR	Median	IQR
IL-1α	7.38	13.305	3.07	6.15	3.63	2.73
IL-1β	66.91	87.77	28.62	67.78	23.81	49.70
IL-10	20.35	20.54	6.88	16.27	8.59	14.58
IL-12p70	13.18	48.29	10.5	78.56	8.35	35.82
IL-18	69.97	29.96	65.3	37.05	52.78	33.12
IL-23	33.83	90.93	25.47	135.87	26.25	128.39
IL-6	35,732	86,525	16,676	20,815	12,344	9356
MCP-1	21,968	9531	12,956	26,666	14,233	10,948
TNF-α	20,837	32,411	12,578	21,118	6841	14,257

MØ, macrophage; TC MØ, TC PEV -treated macrophage; oxTC MØ, oxLDL+TC PEV -treated macrophage; IQR, interquartile range.

2.10. Cytokine analysis with ProcartaPlex immunoassay

Cytokines in the MØ conditioned media were analyzed with ProcartaPlex Multiplex immunoassay (Invitrogen) according to the manufacturer's instructions using a customized panel of 10 cytokines: interleukin (IL)− 1α, − 1β, − 6, − 10, − 12p70, − 15, − 18, − 23, monocyte chemoattractant protein 1/C-C motif chemokine 2 (MCP-1/CCL2), and tumor necrosis factor-α (TNF-α). The conditioned medium samples were measured in duplicates both as non-diluted and 10-fold diluted with a Bio-Plex200 (Bio-Rad) and the data were analyzed using Bio-Plex Manager software. Only concentrations that were within the standard range were used. The culture medium alone was used as a negative control to determine the background and the culture medium with PEVs was used as a control to ensure the absence of targeted cytokines in the PEVs.

2.11. RNAseq

MØ total RNA was isolated with RNeasy Plus kit (Qiagen) according to the manufacturer's instruction, with the exception of one additional wash with the RPE buffer prior to RNA elution. RNA quality and quantity were determined using Nanodrop. Dual-indexed RNA libraries were prepared from 800 ng of total RNA with TruSeq Stranded Total RNA library kit (Illumina, San Diego, CA, USA). Ribo-Zero Globin (Illumina, San Diego, CA, USA) was used for the depletion of cytoplasmic and mitochondrial rRNA as well as globin RNA. Sequencing was performed with NovaSeq 6000 System (Illumina, San Diego, CA, USA). Read length for the paired-end run was 2 × 101 bp and the minimum target read depth of > 30 M paired-end reads for each library. FIMM in-house pipeline (Kumar et al., 2017) was used for the quality evaluation of the RNA sequencing data. Obtained reads were aligned onto the reference genome (GRCh38) by using the STAR (version 2.5.2a).

2.12. Analysis of differentially expressed genes and Functional enrichment analysis

To compute raw counts, the Rsubread Boiconductor package (version 1.34.6) was used and Ensembl release 82 was employed as a reference transcriptome. Once raw counts were extracted for all the samples, lowly expressed genes were filtered out by running a proportion test, as implemented in the NOISeq package (Tarazona et al., 2015). Normalisation and differential expression analysis were performed by using the DESeq2 algorithm (Love et al., 2014). Genes were considered differentially expressed if $\log2FC \leq -0.5$ or $\log2FC \geq 0.5$ and nominal p-value < 0.01. Conversion of gene identifiers was carried out through the use of the biomaRt R package (Durinck et al., 2009). Functional enrichment of differentially expressed genes was performed by using the clusterProfiler Bioconductor package (Yu et al., 2012). The transcriptomic data that support the findings of this study are available in Figshare at https://figshare.com/s/d71a9686497613251465.

2.13. Flow cytometry of macrophages

Cells were stained with anti-CD80-PE (clone 2D10.4, eBioscience), anti-CD86-PE-CF594 (clone 2331/FUN-1, BD Biosciences), anti-CD163-

BV421 (clone GHI/61, BD Biosciences), anti-CD206-APC (clone 19.2, BD Biosciences), anti-HLA-DR-FITC (clone L243, Biolegend) and anti-CD11c-PerCP-Cy5.5 (clone B-ly6, BD Biosciences) according to the manufacturers' instructions. Conjugated isotype control antibodies were used as negative controls for background staining. Prior to staining, MØs were suspended in 50 μl staining buffer (0.3% bovine serum albumin, 2 mM EDTA in PBS, pH 7.2) and incubated with 2.5 μg of Human BD Fc Block™ (BD Pharmingen) for 10 min at RT. The pre-mixed fluorescent antibody cocktail was added, and the cells were incubated on ice in darkness for 30 min. After staining, the cells were washed with 2 ml staining buffer, pelleted by centrifuging at 350 g for 10 min, and suspended in 100 μl staining buffer. Cell data were acquired with BD FACSAria IIU (BD Biosciences) flow cytometer using FACSDiva™ software (v8.0.1; BD Biosciences) and analyzed with FlowJo™ software (v10.0.7; FlowJo, LLC). MØs were gated based on forward (FSC) and side (SSC) scatter patterns. Doublets and aggregates were excluded using FSC-area versus FSC-height. The fluorescence-positive cells were gated based on isotype controls and populations. The results are presented as median fluorescence intensity (MFI) and frequency of positive cells. The representative scatter plots and histograms as well as the gating strategy are presented in Supplementary Fig. A.2.

2.14. Statistical analysis

Statistical analyses were performed using GraphPad Prism (v9.0.2; GraphPad Software Inc.). Normality of the data was determined by the Shapiro-Wilk test and when passed, differences between the groups were determined using the appropriate parametric tests. Otherwise, appropriate non-parametric tests were used. The test used is indicated in the figure legends. $p < 0.05$ was considered statistically significant.

2.15. Ethics approval

This study was conducted in line with the ethical principles of the Declaration of Helsinki. All used platelet concentrates, buffy coats, and plasma were handled anonymously, and only material that could not be administered clinically was used as accepted by the Finnish Supervisory Authority for Welfare and Health (Valvira, Finland). All blood donors had given informed consent for the use of the surplus material in research. There was no possibility to trace blood donors to the samples used and no personal data of any kind was possible to link to the cells or blood material used in this study. All samples were destroyed after this study.

3. Results

3.1. OxLDL potentiates the release of PEVs from thrombin and collagen co-stimulated platelets, but not from unstimulated platelets

To prepare state-of-the-art oxLDL for studying PEV production, freshly isolated LDL from human plasma was incubated with copper sulfate and LDL oxidation was confirmed by measuring the TBARS before and after the incubation (Supplementary Fig. A.3). Platelets were incubated with oxLDL, after which the concentration of PEVs, identified by the expression of CD61, the subunit of CD41/CD61 integrin complex (platelet glycoprotein IIb/IIIa/integrin αIIbβ3), a prominent platelet marker, was measured by Apogee A-50 from the supernatants, which were carefully ensured to be platelet-free. Compared to unstimulated platelets, oxLDL alone did not significantly increase the concentration of $CD61^+$ EVs (Fig. 1A). However, there was a large inter-donor variation between the responses within the eight biological replicates (platelets derived from 32 donors). We next investigated whether oxLDL could potentiate PEV production of activated platelets by using T and C activation, the combined effect of which on the PEV production is well known (Aatonen et al., 2014). An increase in the concentration of $CD61^+$ EVs from oxLDL+TC stimulated platelets was seen already after 1 h compared to TC-stimulated platelets, and the potentiating effect continued at 3- and 5-h time points (Supplementary Fig. A.4). Since PEVs started to form from unstimulated platelets at 5 h, we chose to use 3-h activation (2.5-h preincubation with oxLDL followed by stimulation by TC for 30 min) in the subsequent experiments to maximize the number of specifically induced PEVs. When platelets were stimulated by TC alone, the concentration of $CD61^+$ EVs in the platelet-free supernatant was on average 4-fold compared to the unstimulated controls (Fig. 1B). When platelets were sensitized with oxLDL prior to the TC stimulation, the concentration of $CD61^+$ EVs was on average 2-fold compared to the TC-stimulated platelets (Fig. 1B). Our data demonstrates that oxLDL could significantly enhance PEV formation only of activated, but not resting platelets. When the platelets were treated with (non-oxidized) LDL at the same concentration and for the same time as with oxLDL, followed by the TC stimulation, no increase in the concentration of $CD61^+$ EVs was detected compared to the TC stimulation only (Supplementary Fig. A.5).

The effect of oxLDL pretreatment on the number of TC-induced

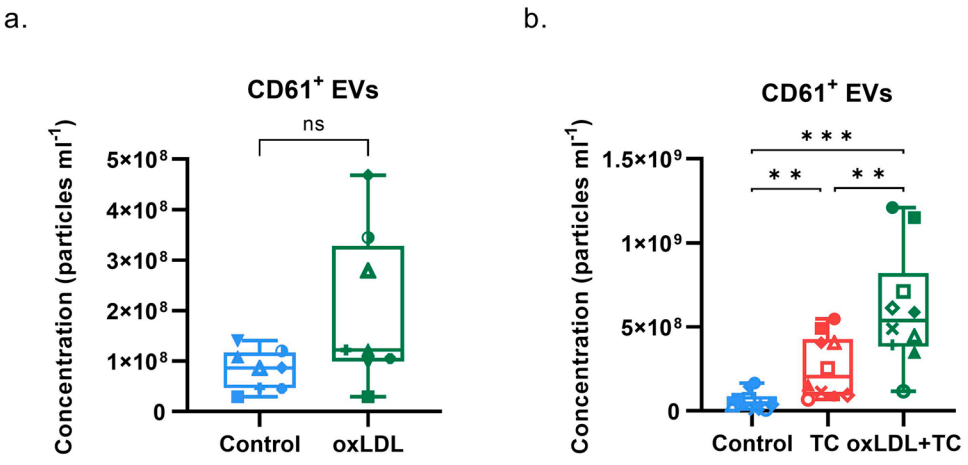

Fig. 1. Concentration of $CD61^+$ EVs from unstimulated and stimulated platelets. SEC-isolated platelets were stimulated by oxLDL alone or by TC with or without oxLDL pre-sensitization, after which platelets were carefully removed, and EVs in the platelet-free supernatants were stained with PE-conjugated mouse anti-human CD61 and analyzed by high-sensitivity flow cytometer from oxLDL-stimulated (A) and TC- and oxLDL + TC-stimulated (B) platelets. As a control for constitutive EV release, EVs were measured from the platelet-free supernatant of unstimulated platelets. The results represent $CD61^+$ EVs with a size range of 200–1000 nm and exceeding the fluorescence gate. The interquartile range (box), median (line within the box), and the min to max range (whiskers) with data points are shown. N = eight biological replicates (A) and ten biological replicates (B). Each biological replicate is a pool of platelets from four donors. Differences between the groups were determined by the paired t test (A) or the repeated measures one-way ANOVA with the Tukey's multiple comparison test (B). * *$p < 0.01$; * **$p < 0.001$; ns, not significant; SEC, size-exclusion chromatography; PE, phycoerythrin; LDL, low-density lipoprotein; oxLDL, oxidized low-density lipoprotein; T, thrombin; C, collagen.

procoagulant and adhesive PEVs was analyzed by lactadherin (a PS-binding protein)-FITC and anti-CD62P (P-selectin)-PE staining by flow cytometry. Supporting what was observed with $CD61^+$ EVs, an increase in PEV numbers was also seen by $lactadherin^+$ and $CD62P^+$ EVs. Activation of platelets by TC alone increased the concentration of $lactadherin^+$ EVs on average by 1.5-fold compared to unstimulated platelets, and induced the release of $CD62P^+$ EVs that were not detected in the supernatants of unstimulated platelets (Supplementary Fig. A.6). Compared with TC only, oxLDL pretreatment further increased the concentration of TC-induced $lactadherin^+$ and $CD62P^+$ EVs by on average 1.7- and 1.8-fold, respectively (Supplementary Fig. A.6). Based on median fluorescence intensity (MFI), there was no difference in the PS or P-selectin expression levels between the oxLDL+TC-induced and TC-induced PEVs (Supplementary Fig. A.6), showing that oxLDL increased EV numbers rather than PS- and P-selectin expression.

The potentiating effect of oxLDL on TC-induced PEV formation was also analyzed by NTA from UC-isolated PEV samples. The number of particles from the oxLDL+TC-stimulated platelets was on average 1.7-fold compared to that from the TC-stimulated platelets, but the difference was not statistically significant (Supplementary Fig. A.7). No significant difference was seen in the mean or mode sizes between the oxLDL+TC- and TC-induced UC-isolated PEVs, both being slightly bigger in diameter compared to the PEVs from control platelets (Supplementary Fig. A.7). The absence of lipoproteins, potential co-sedimenting non-EV particles, in the PEV isolates was confirmed by western blot of apoB, the major protein constituent of LDL, which showed that the majority of the exogenous lipoproteins in the PEV samples had been removed during the UC-isolation (Supplementary Fig. A.8.).

3.2. Blocking CD36, but not the Toll-like receptor 4, suppresses the potentiating effect of oxLDL on the TC-induced PEV production

Next, we analyzed the effect of blocking CD36 and TLR4, receptors known to mediate oxLDL interactions in cells (Levitan et al., 2010), on the oxLDL+TC-induced PEV production. Pre-incubation of platelets with an anti-CD36 decreased the concentration of oxLDL+TC-induced $CD61^+$ EVs on average by 50% (Fig. 2). In contrast, the concentration of oxLDL+TC-induced $CD61^+$ EVs was not decreased when platelets were pre-incubated with anti-TLR4, nor was there any further inhibition when both CD36 and TLR4 were blocked. Thus, the data suggest that the oxLDL-dependent increase in the formation of TC-induced PEVs was largely dependent on CD36.

We further tested the effect of HDL, a physiologically relevant CD36-binding molecule (Calvo et al., 1998; Connelly et al., 1999) which has anti-atherosclerotic properties, on oxLDL+TC-induced PEV formation. When HDL (50 μg/ml) was added to platelets at the same time as oxLDL, the concentration of oxLDL+TC-induced $CD61^+$ EVs reduced on average by 24% (Fig. 3A), whereas pre-incubation of platelets with doubled HDL concentration (100 μg/ml) 30 min prior to oxLDL addition reduced the concentration of oxLDL+TC-induced $CD61^+$ EVs by 30% (Fig. 3B). Although, not statistically significant, the data implies that HDL may suppress the effect of oxLDL on PEV formation from activated platelets.

3.3. Characterization of EV markers on oxLDL+TC- and TC-induced PEVs

To characterize and compare the formed PEVs, selected EV-marker proteins were analyzed by western blot. The PEVs from oxLDL+TC- and TC-activated platelets equally expressed the prominent platelet integrin CD41 subunit and canonical EV markers CD63, CD9, TSG101, whereas the endoplasmic reticulum resident protein calnexin was richly present in platelets, but not detectable in the PEVs (Supplementary Fig. A.8). Transmission electron microscopy displayed PEVs of typical morphology, but no lipoproteins (Supplementary Fig. A.8), supporting the western blot showing that apoB-100 was removed during PEV isolation (Supplementary Fig. A.8).

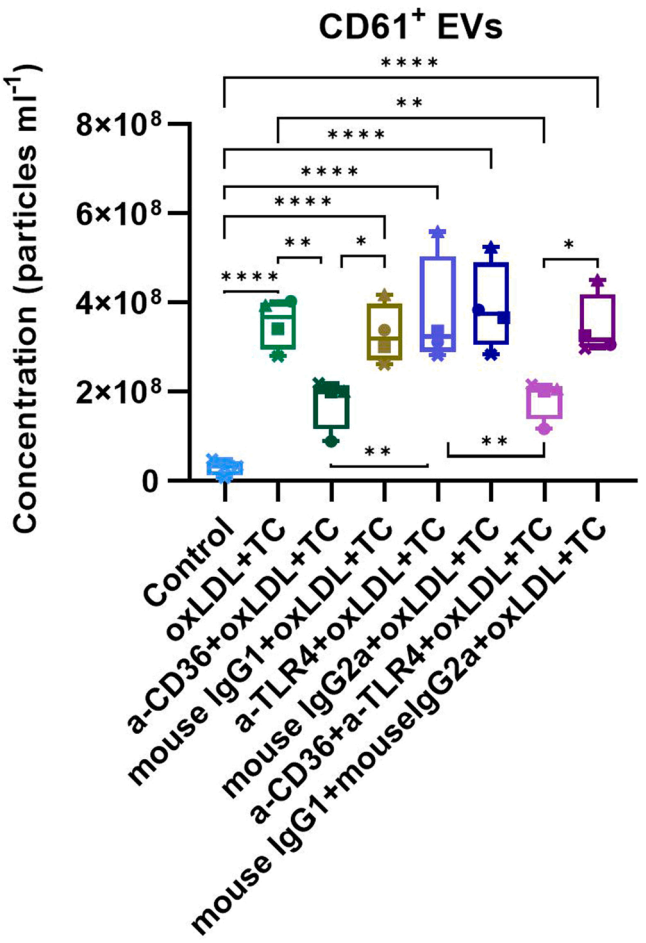

Fig. 2. Concentration of oxLDL+TC-induced $CD61^+$ PEVs in the presence and absence of CD36 and TLR4 receptor-blocking antibodies. SEC-isolated platelets were preincubated with an anti-CD36, anti-TLR4, or their combination, then presensitized with oxLDL and finally stimulated by TC. Isotype-matched immunoglobulins were used as negative controls. After activation, platelets were carefully removed and EVs in the platelet-free supernatants were stained with PE-conjugated anti-CD61 and analyzed by flow cytometry. As a control for constitutive EV release, EVs were measured from the platelet-free supernatants of unstimulated platelets. The results represent $CD61^+$ EVs with a size range of 200–1000 nm and exceeding the fluorescence gate. The interquartile range (box), median (line within the box), and the min to max range (whiskers) with data points are shown. N = four biological replicates. Each biological replicate is a pool of platelets from four donors. Differences between the groups were determined by the Friedman test with the Dunn's multiple comparison test. Of note, only the most relevant statistically significant differences are shown in the figure for clarification. *$p < 0.05$; **$p < 0.005$; ***$p < 0.001$; ****$p < 0.0001$ oxLDL, oxidized-low-density lipoprotein; T, thrombin; C, collagen; TLR4, toll-like receptor 4; PE, phycoerythrin; SEC, size exclusion chromatography.

3.4. The inflammatory protein content of PEVs is altered by platelet activation

Prompted by our previous observations on agonist-dependent cargo variability of PEVs (Aatonen et al., 2014), the cargo of inflammatory proteins in the UC-isolated oxLDL+TC- and TC-induced as well as control PEVs was analyzed by PEA. Of the 92 inflammation-related proteins targeted (Supplementary Table A.1), 29 were found in all three PEV types (Fig. 4A). Six proteins IL8/CXCL8, IL7, MCP-1/CCL2, TNF-related apoptosis-inducing ligand (TRAIL), CCL4, and extracellular newly identified receptor for advanced glycation end-products (EN-RAGE)

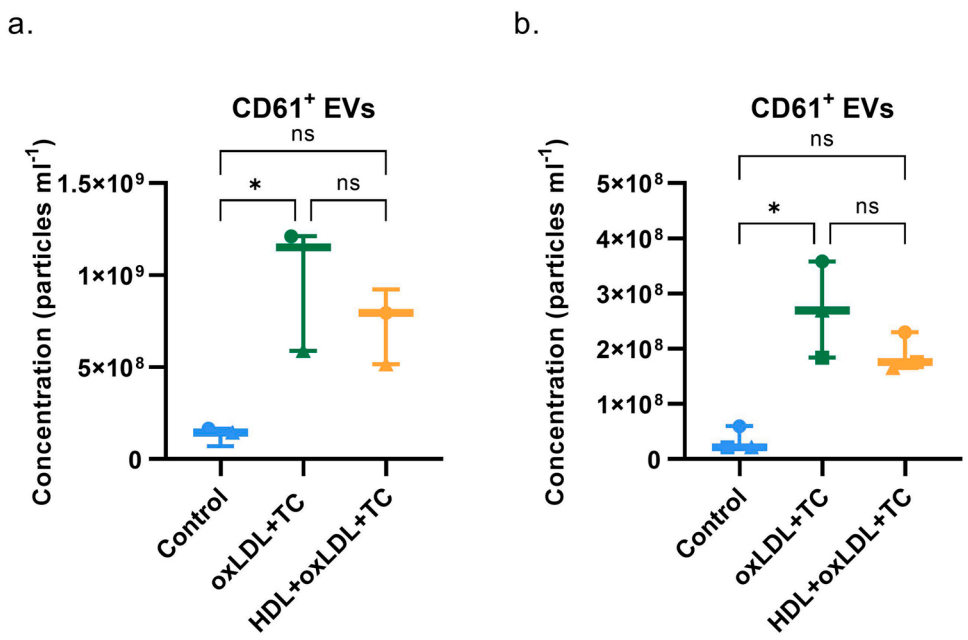

Fig. 3. Concentration of oxLDL+TC-induced CD61$^+$ PEVs in the presence and absence of HDL. SEC-isolated platelets were presensitized with oxLDL in the presence and absence of 50 μg/ml (A) and 100 μg/ml (B) HDL and finally stimulated by TC. HDL was added to platelets either at the same time as oxLDL (A) or 30 min prior to oxLDL (B). After activation, platelets were carefully removed and EVs in the platelet-free supernatants were stained with PE-conjugated anti-CD61 and analyzed by flow cytometry. As a control for constitutive EV release of EVs, EVs were measured from the platelet-free supernatants of non-stimulated platelets. The results represent CD61$^+$ EVs with a size range of 200–1000 nm and exceeding the fluorescence gate. Median and range with data points are shown. N = three biological replicates. Each biological replicate is a pool of platelets from four donors. Differences between the groups were determined by the Friedman test with the Dunn's multiple comparison test.* $p < 0.05$ HDL, high-density lipoprotein; oxLDL, oxidized-low-density lipoprotein; T, thrombin; C, collagen; PE, phycoerythrin; SEC, size exclusion chromatography; ns, not significant.

were only detected in the PEVs from unstimulated platelets (Fig. 4A), indicating differential cargo packaging between the PEVs of stimulated and unstimulated platelets. No proteins were found to be exclusively present in the PEVs of TC-stimulated or oxLDL+TC-stimulated platelets, and no statistically significant differences were detected in the protein expression levels between these two PEV types (Fig. 4A & B). Instead, a clearer difference in the protein expression levels was found between the PEVs from unstimulated and stimulated platelets. A total of 14 of the analyzed proteins were upregulated and 11 proteins downregulated in the PEVs from stimulated compared to unstimulated platelets (Fig. 4B). The expression levels of four proteins, ST1A1, IL18, growth-regulated alpha protein/CXCL1, and latency-associated peptide transforming growth factor (LAP TGF)-β1 were significantly different between the PEVs from oxLDL+TC-stimulated and unstimulated platelets, and of these, ST1A1 and IL18 were upregulated, whereas CXCL1 and LAP TFG-β1 were downregulated in the oxLDL+TC-induced PEVs (Fig. 4B). Principal component analysis showed that the oxLDL+TC- and TC-induced PEVs clustered together, whereas PEVs from unstimulated platelets formed another cluster (Fig. 4C) supporting the observation that the inflammatory protein content of the PEVs from oxLDL+TC--stimulated and TC-stimulated platelets did not significantly differ.

3.5. PEVs from the oxLDL+TC- and TC-activated platelets modulate macrophage phenotype

To investigate, whether the oxLDL+TC- or TC-induced PEVs could affect proinflammatory MØ differentiation, human PBMC-derived monocytes were differentiated into M1-like MØs in the presence or absence of PEVs, followed by activation with IFN-γ and LPS in the presence or absence of PEVs (Fig. 5A). MØ surface markers were then analyzed by flow cytometry. Compared to the control MØs differentiated and activated towards M1 in the absence of PEVs, the presence of PEVs induced a significant increase in the HLA-DR expression (both MFI and frequency of positive cells) and CD86 expression (frequency of positive cells) (Fig. 5B). In general, no differences were detected in the analyzed surface markers between the oxLDL+TC PEV-treated MØs and TC PEV-treated MØs (oxTC MØ and TC MØ, respectively). However, treatment of the MØs with the TC-induced PEVs, but not oxLDL+TC-PEVs, significantly decreased the frequency of CD11c$^+$ MØs compared to control MØs (Fig. 5B).

3.6. OxLDL+TC- and TC-induced PEVs alter the cytokine secretion of macrophages

To analyze the ability of PEVs to modulate the inflammatory response of the MØs selected cytokines/chemokines in the MØ conditioned media were analyzed. From the 10 analytes targeted (IL1α and − 1β, IL10, IL12p70, IL18, MCP-1/CCL2, TNF-α, IL6, IL23, and IL15), all but one (IL15), were detected in the conditioned media. The presence of PEVs during the MØ differentiation and activation significantly decreased the secretion of proinflammatory cytokines IL6 and IL12p70 (IL12p70 only with TC-induced PEVs). A trend of decreased secretion was also seen with other proinflammatory cytokines, namely IL1α and − 1β, TNF-α, and IL18, as well as MCP-1/CCL2, but also with anti-inflammatory cytokine IL10 (Fig. 6). In contrast, a trend of increased secretion was observed with IL-23. In the absence of PEVs, the highest concentration was detected for IL6 followed by MCP-1/CCL2 and TNF-α, whereas IL1α was secreted at the lowest level (Table 1). However, a large biological variation was observed between the MØs from 11 donors.

3.7. OxLDL+TC- and TC-induced PEVs differently modulate the transcriptome of macrophages

Finally, we analyzed the gene expression of the PEV-treated MØs and control MØs by performing RNA sequencing followed by differential gene expression and over-representation analyses. No differences were observed in the gene expression of the prototypic markers of the MØ polarization types such as M1, M2, M4, or Mreg [reviewed in (De Sousa et al., 2019)]. Although the gene expression profiles of MØs clustered together more based on the donor than the treatment (Fig. 7A), differences were exhibited in the gene signatures between the control MØs and the PEV-treated MØs. A total of 234 and 115 differentially expressed genes (DEGs) were detected between the TC MØs vs. control MØs and between the oxTC MØs vs. control MØs, respectively, whereas only one DEG was found between the TC vs. the oxTC MØs (Supplementary Tables A.2-A.4). Of these, 143 DEGs were exclusive to TC MØs vs. control MØs and 24 DEGs to oxTC MØs vs. control MØs, whereas 91 DEGs were shared between the oxTC MØs vs. control MØs and TC MØs vs. control MØs (Fig. 7B). Thirty pathways were significantly over-represented in the 143 DEGs exclusive to the TC MØs vs. control

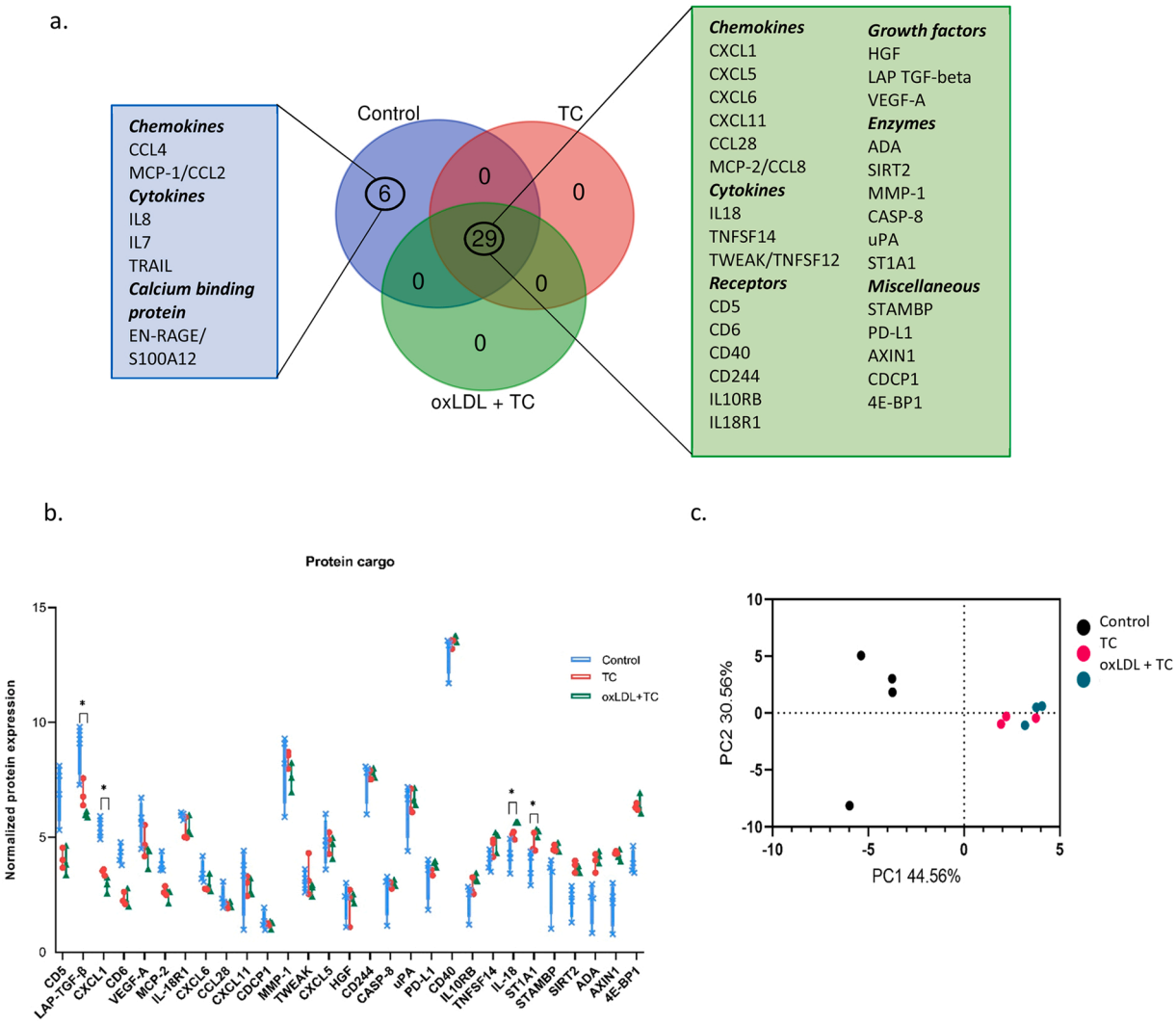

Fig. 4. Inflammatory protein content of the PEVs. UC-isolated PEVs from the oxLDL+TC- and TC-stimulated platelets and unstimulated control platelets were subjected to the proximity extension assay to target 92 inflammation-related proteins. Overlap of the detected proteins across the three PEV types is presented by Venn diagram (A). The expression of the 29 proteins found in all PEVs is shown as Normalized Protein eXpression (NPX) values calculated from Ct values (B). The interquartile range (box), median (line within the box), and the min to max range (whiskers) with data points are shown. N = three (TC and oxLDL+TC) and four (control) biological replicates. Each biological replicate represents a pool of platelets from four donors. Of note, a protein was judged to be expressed in the PEVs if it was detected in two out of three biological replicates (TC and oxLDL + TC), or three out of four biological replicates (control). Differences between the groups were determined by the Kruskall-Wallis test with the Dunn's multiple comparison test. *$p < 0.05$. The clustering of the different PEV types are shown by principal component analysis plot (C). ns, not significant; UC, ultracentrifugation; oxLDL, oxidized low-density lipoprotein; T, thrombin; C, collagen.

MØs, many of which were associated with cell cycle and regulation of gene expression (Fig. 7B). The five significantly over-represented pathways in the 24 DEGs exclusive to the oxTC MØs vs. control MØs were associated with the immune system such as chemokine and interleukin signaling (Fig. 7B). In the 91 DEGs shared between oxTC MØs vs. control MØ sand TC MØs vs. control MØs, 26 pathways were significantly over-represented including pathways associated with cell cycle and DNA replication (Fig. 7B). Based on these data, stimulation of platelets by TC seemed to be the main driver for the differences in gene expression between the PEV-treated and control MØs. Interestingly, none of the pathways related to the cell cycle and regulation of gene expression (such as chromatin remodeling and transcriptional regulation) that were over-represented in the DEGs between the TC MØs vs. control MØs were over-represented in the DEGs between the oxTC MØs vs. control MØs. Instead, the oxLDL presensitization of platelets prior to TC-stimulation seemed to produce PEVs that were able to shift transcription toward genes involved in immune system-related functions such as chemokine and interleukin signaling.

4. Discussion

In this study, we show that oxLDL increased the formation of PEVs, when the oxLDL-pretreated platelets were activated with TC co-stimulus. The potentiating effect of oxLDL was largely suppressed by blocking the platelet CD36, but not by blocking TLR4. This result is in line with previous studies showing that activation by oxLDL via CD36 results in platelet expression of P-selectin, PS, and the activated conformation of the CD41/CD61 (Nergiz-Unal et al., 2011; Yang et al., 2018). The effects of oxLDL activation can now be extended to also include PEV formation, but only when an auxiliary activator is present. Furthermore, also in line with the previous studies showing that HDL is able to blunt platelet activation (Ardlie et al., 1989; Takahashi et al., 1996) and to reduce time-dependent PEV formation in therapeutic platelet concentrates (Pienimaeki-Roemer et al., 2014), we observed that HDL blunted the formation of PEVs from oxLDL+TC-stimulated platelets. Since HDL also binds to CD36 (Calvo et al., 1998; Connelly et al., 1999), it possibly competes for the CD36 binding sites,

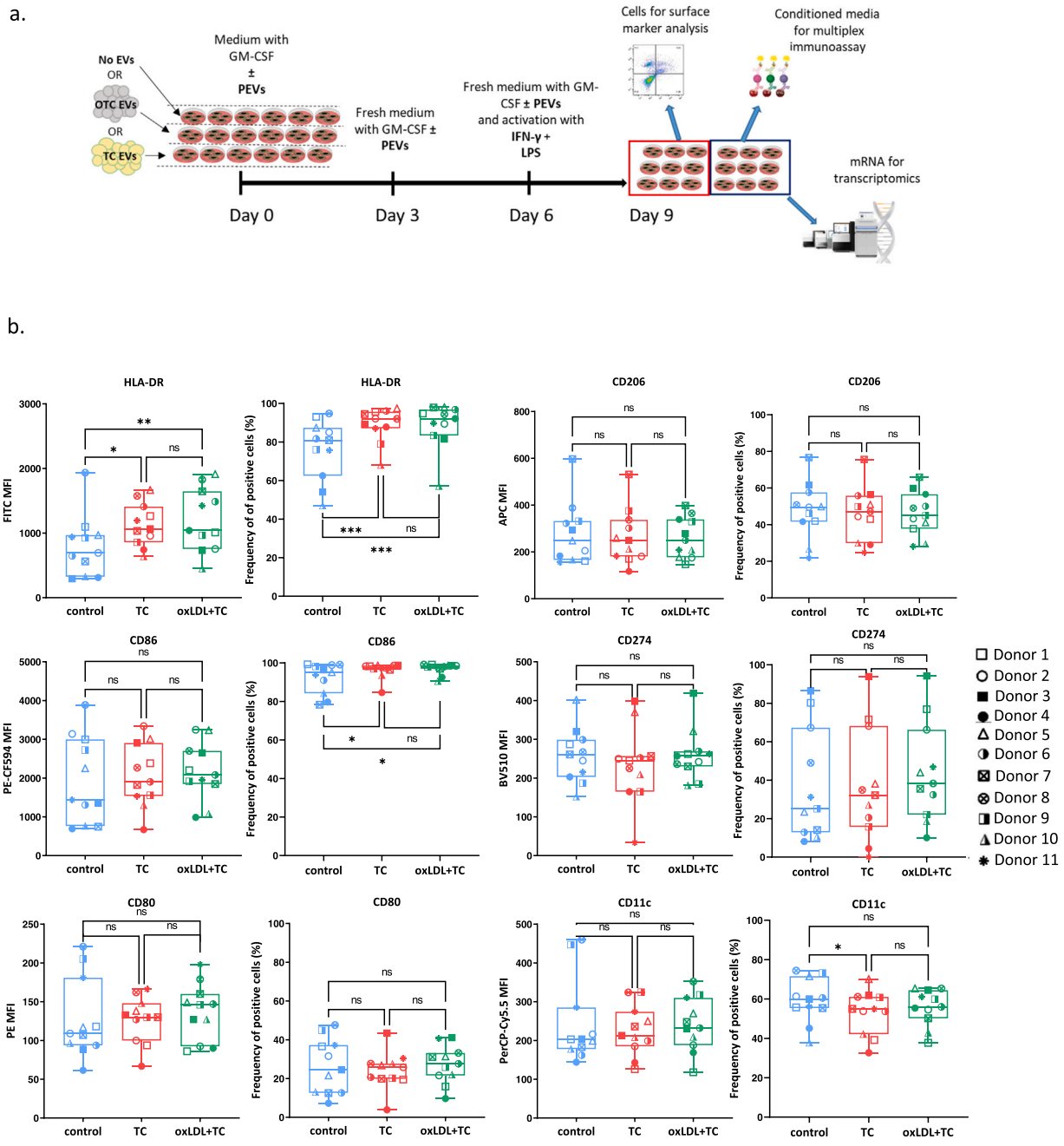

Fig. 5. Flow cytometry of the surface markers of MØs differentiated and activated in the presence and absence of PEVs. The MØs were differentiated from PBMCs for six days under GM-CSF with oxLDL+TC- induced PEVs or TC-induced PEVs or without PEVs (control) and then activated with IFN-γ and LPS for three days with or without the PEVs (A). After the activation, the indicated surface markers on the MØs were analyzed by flow cytometry (B). The results are presented as MFI and frequency of positive cells. The interquartile range (box), median (line within the box), and the min to max range (whiskers) with data points are shown. N = 11 biological replicates (= different MØ donors). Differences between the groups were determined by the repeated measures one-way ANOVA with the Tukey's multiple comparison test. *p < 0.05; * *p < 0.005; ***p<0.0005. ns, not significant; MØ, macrophage; PBMC, peripheral blood-derived mononuclear cell; MFI, median fluorescence intensity; oxLDL, oxidized low-density lipoprotein; T, thrombin; C, collagen; GM-CSF, granulocyte-macrophage colony-stimulating factor; IFN-γ, interferon-γ; LPS, lipopolysaccharide.

diminishing PEV formation. Taken together, the present data support a novel, CD36-mediated role for oxLDL in the formation of PEVs from activated platelets.

The oxLDL-mediated increase in the formation of TC-induced PEVs was identified by CD61, a prominent platelet marker, but the effect of oxLDL was also reflected as increased numbers of PS^+ and P-selectin$^+$ EVs, suggesting that the availability of procoagulant surface and leukocyte contact points were enhanced by oxLDL. The analytical strategy to detect ($CD61^+$) EVs from the platelet-free supernatant by flow cytometry was chosen for two reasons: 1) the ability to discriminate EVs from non-EV particles such as lipoproteins based on immunofluorescence and 2) to avoid EV isolation, which could lead to loss of subpopulations or cause clumping/destruction of the EVs. However, since the used flow cytometer only detects vesicles ≥ 200 nm (based on the light scatter calibration with Rosetta beads and software from Exometry, The Netherlands), the effect of oxLDL on PEV production from TC-stimulated platelets was also confirmed by NTA that detects < 200 nm EVs.

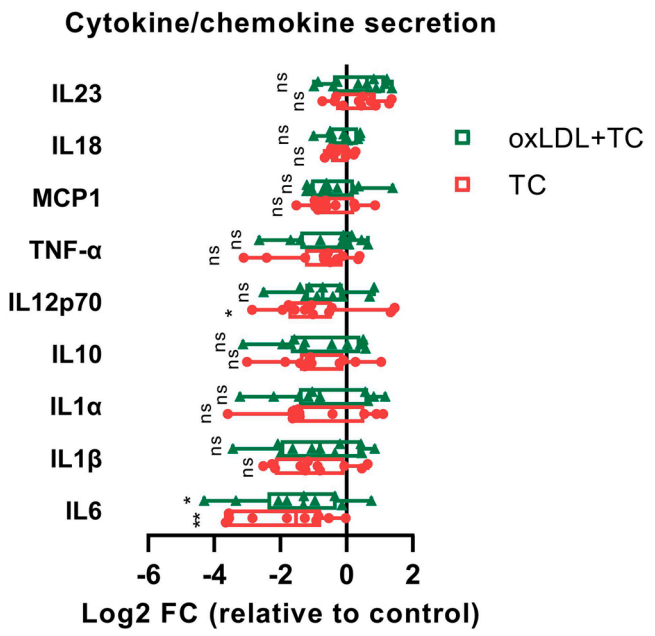

Fig. 6. Cytokines and chemokines secreted by the MØs differentiated and activated in the presence and absence of PEVs. The MØs were differentiated from PBMCs for six days under GM-CSF with oxLDL+TC- induced PEVs or TC-induced PEVs or without PEVs (control) and then activated with IFN-γ and LPS for three days with and without the PEVs. After the activation, the MØ-conditioned media were collected and the concentrations of the indicated cytokines and chemokines were analyzed from the conditioned media by a multiplex immune assay. The results are presented as Log2 fold changes relative to the control MØs. The interquartile range (box), median (line within the box), and the min to max range (whiskers) with data points are shown. N = 11 biological replicates (= different MØ donors). Differences between the groups were determined by the Friedman test with the Dunn's multiple comparison test. *p < 0.05; * *p < 0.005; ns, not significant; MØ, macrophage; PBMC, peripheral blood mononuclear cell; GM-CSF, granulocyte-macrophage colony-stimulating factor; oxLDL, oxidized low-density lipoprotein; T, thrombin; C, collagen; IFN-γ, interferon-γ; LPS, lipopolysaccharide; IL, interleukin; MCP-1, monocyte chemoattractant protein-1; TNF-α, tumor necrosis factor-α.

The two previous studies on the effect of oxLDL on PEV formation (Wang et al., 2012; Nielsen et al., 2015) displayed contradictory results, which can now be explained by this study where contemporary EV analytics were used with special attention to platelet handling and the used lipoproteins. Platelets are easily activated by auto-activating substances such as ADP, and PEV formation can also be induced in vitro by a variety of factors including time (platelet storage), mechanical shearing and low temperature (Boilard et al., 2015; Taus et al., 2019). Thus, a primed state, in which platelets have been sensitized for increased responsiveness may be inadvertently generated during platelet handling, which can then be augmented to produce PEVs by a weak platelet activator normally deficient on its own, such as oxLDL. In the study by Nielsen and coworkers (Nielsen et al., 2015), where platelet sensitization was well controlled, neither oxLDL or LDL promoted PEV formation, similar to our results. As suggested by the large variability in responses to oxLDL alone (Fig. 1A), we may have not been able to fully avoid platelet sensitization/priming during handling or the platelets may have already been in a primed state in the concentrates, and thus we chose to compare the effect of oxLDL on TC-stimulated platelets, which also resembles more the proatherogenic conditions.

Increased numbers of PEVs have previously been observed in patients with atherosclerosis with a positive correlation between the numbers of circulating PEVs and the disease state (Kuriyama et al., 2010; Lukasik et al., 2013; Suades et al., 2015). In atherosclerosis settings, T and C are classical platelet agonists leading to strong platelet activation e.g. at the site of atherosclerotic plaque rupture. However, plasma cholesterol levels (Carvalho et al., 1974; Harmon et al., 1986) and modified lipoproteins (Podrez et al., 2007; Berger et al., 2020) impact platelets' sensitivity to activation by priming platelets for increased responsiveness to agonists. Furthermore, during aging, a sensitized state of platelets seems to emerge [reviewed in (Faria et al., 2020)] potentially due to age-dependent inflammatory and metabolic changes (Davizon-Castillo et al., 2019). A sensitized or hyper-reactive state of platelets (Van Der Meijden, Heemskerk, 2019) could be a critical factor enabling enhanced PEV formation in vivo. Since oxLDL is present in the plasma of atherosclerosis patients and in atherosclerotic plaques of both humans and experimental animals (Yla-Herttuala et al., 1989; Yla-Herttuala et al., 1990; Steinberg and Witztum, 2010; Lehti et al., 2018), platelets may encounter oxLDL in vivo in circulation or in the atherogenic intima resulting in sensitization of platelets for increased responsiveness to subsequent agonists, such as T and/or C (Davi et al., 1998; Colas et al., 2011; Biswas et al., 2017; Berger et al., 2020).

Also, the characteristics of PEVs are thought to change during disease states (Aatonen et al., 2012; Puhm et al., 2021). Platelets have been shown to dynamically alter the cargo of the PEVs depending on the activating stimuli (Baj-Krzyworzeka et al., 2002; Aatonen et al., 2014; Ferreira et al., 2020; Suades et al., 2022) and thereby to appropriately respond to the (patho)physiological state of the microenvironment. However, the molecular composition of the PEVs from oxLDL+TC-activated platelets was surprisingly similar to that of the PEVs from TC-activated platelets regarding the expression of PS and P-selectin and the cargo of the targeted inflammation-related proteins. We hypothesize that the strong platelet activation by TC may have masked the signaling pathways activated by the "weaker" oxLDL stimulus.

PEVs have the ability to regulate immune cell differentiation and reactivity by e.g. altering cells' phenotype and inflammatory response (Sadallah et al., 2011; Sadallah et al., 2014). Therefore, we investigated the capacity of the oxLDL+TC- and the TC-induced PEVs to modulate phenotypic, functional, and transcriptomic signatures of MØs, the key inflammatory cells in atherosclerosis. We used a previously established protocol for differentiating PBMCs into M1-like MØs (Hyvärinen et al., 2018) and treated the MØs with PEVs for the duration of their differentiation and activation phases. Both PEV types boosted the M1-like phenotype by increasing HLA-DR and CD86 expression, and decreased the expression of CD11c. Furthermore, both PEV types increased the secretion of proinflammatory cytokine IL23, a classical M1 marker, and decreased the secretion of IL10, an anti-inflammatory cytokine often associated with the M2 phenotype [reviewed in (Martinez and Gordon, 2014)]. In contrast to IL-23, both PEV types decreased the secretion of several other proinflammatory cytokines (IL6, TNF-α, IL12p70, and IL1β) as well as MCP-1/CCL2. Thus, in this experimental model PEVs promoted some and quenched some proinflammatory properties of MØs resulting in a mixed MØ phenotype which is in agreement with the current view that MØs exhibit a wide spectrum of phenotypes including combined phenotypes having features of both M1 and M2 (Soldano et al., 2018; Trombetta et al., 2018; De Sousa et al., 2019). In the context of atherosclerosis and platelets, of particular interest is the M4 phenotype induced by CXCL4, a chemokine abundant in PEVs (Baj-Krzyworzeka et al., 2002; Dean et al., 2009). The prevalence of the M4 phenotype in atherosclerotic arteries has been associated with the plaque instability in human and experimental animal studies (Erbel et al., 2015), and knocking out the Pf4 gene in Apoe−/− mice was reported to lead to reduced atherosclerotic lesion formation (Sachais et al., 2007). The observed phenotypic changes (overexpression of CD86 and HLA-DR as well as low phagocytic activity portrayed by the decrease in $CD11c^{+}$ cells) could potentially also be associated with the M4 (Gleissner et al., 2010). Of note, we have confirmed the presence of CXCL4 in our TC-induced PEVs by proteomics (Palviainen et al., unpublished data).

Based on the transcriptome analysis, the gene expression of the PEV-treated MØs differed clearly from the M1-like control MØs. Pathways involved in the cell cycle and regulation of gene expression (such as

a.

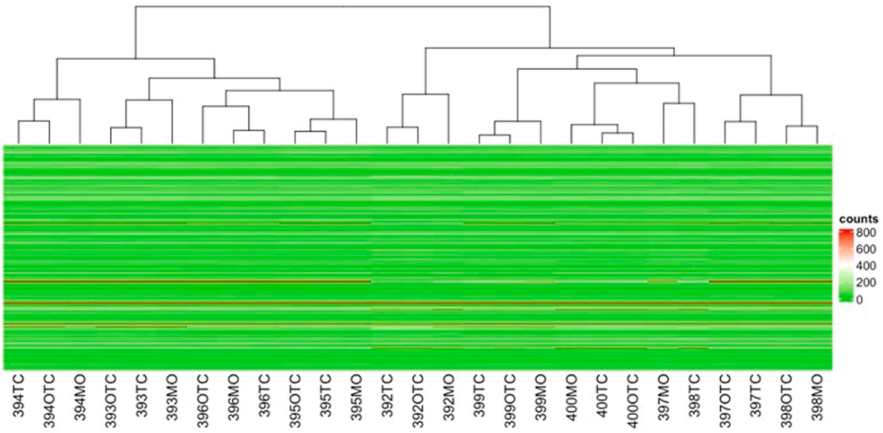

b.

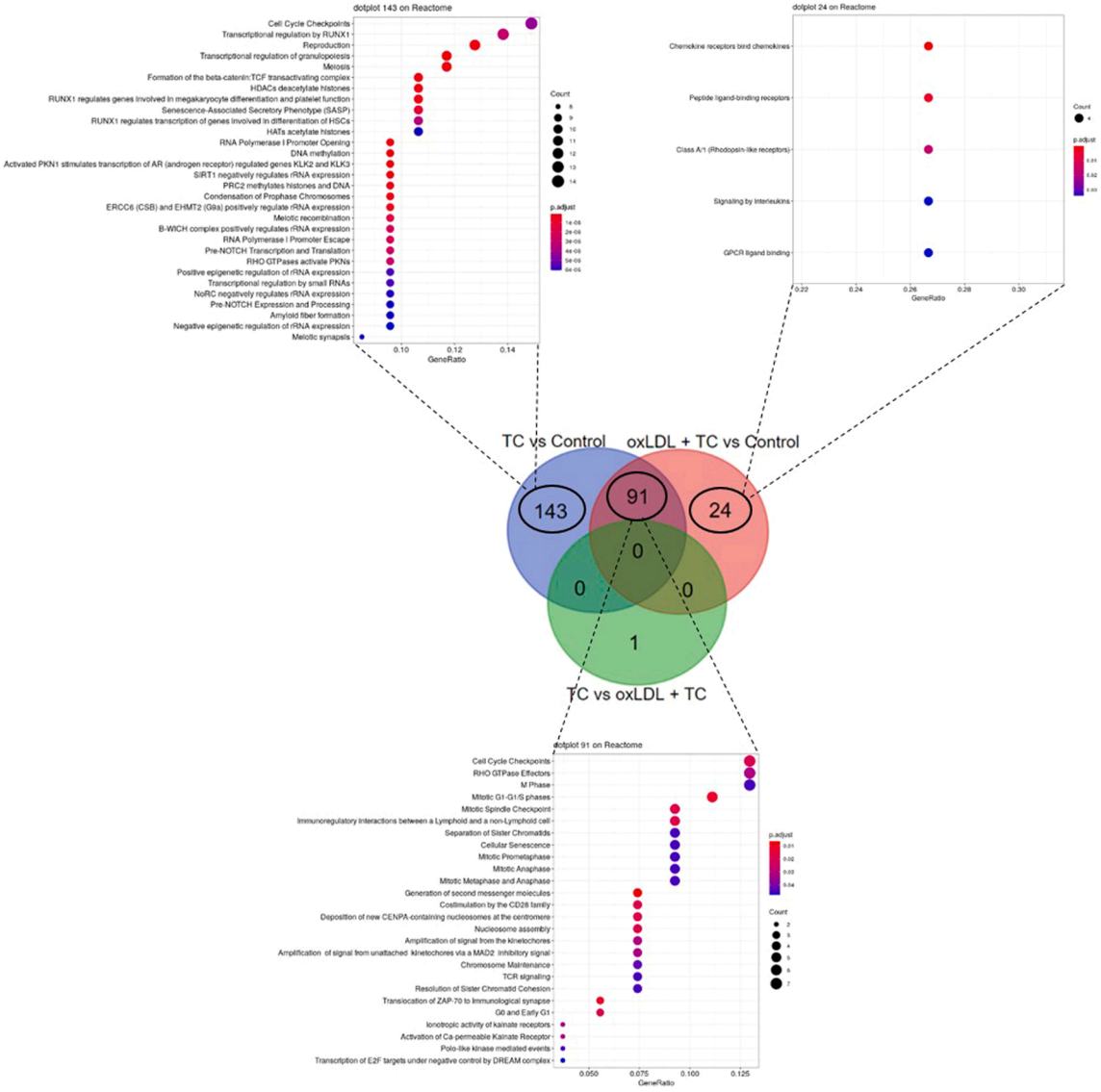

(caption on next page)

Fig. 7. Differentially expressed genes (DEGs) and over-represented pathways in the DEGS between PEV-treated and non-treated MØs. MØs were differentiated from the PBMCs for six days under GM-CSF with oxLDL+TC- induced PEVs or TC-induced PEVs or without PEVs (control) and then activated with IFN-γ and LPS for three days with and without the PEVs. After activation, the MØ mRNA was isolated and subjected to RNASeq and differential gene expression analysis. A heatmap of the read counts with a clustering of the samples (A). Venn diagram showing overlap of DEGs, filtered based on $p < 0.01$ and Log2 fold change ≤ 0.5 or ≥ 0.5, between the three comparisons and the dot plots showing significantly over-represented pathways (adjusted p value < 0.05) in DEGs exclusive to TC MØs vs. control MØs and to oxTC MØs vs. control MØs, and in the DEGs shared between the TC MØs vs. control MØs and the oxTC MØs vs. control MØs (B). N = nine biological replicates (= MØ donors). PBMC, peripheral blood mononuclear cell; GM-CSF, granulocyte-macrophage colony-stimulating factor; oxLDL, oxidized low-density lipoprotein; T, thrombin; C, collagen; IFN-γ, interferon-γ; LPS, lipopolysaccharide; DEG, differentially expressed gene; TC MØ, macrophage treated with TC-induced PEVs; oxTC MØ, macrophage treated with oxLDL+TC-induced PEVs.

transcriptional regulation, epigenetic modification, and chromatin remodeling) were significantly over-represented in the DEGs between the TC MØs vs. control MØs, whereas pathways associated with immune system -related functions (chemokine and cytokine signaling) were significantly over-represented in the DEGs between oxTC MØs vs. control MØs. Based on the shared DEGs, we postulate that the TC-induced properties of the PEVs were mainly responsible for the differences in gene expression between the PEV-treated and control MØs, and that the impact of oxLDL was more to fine-tune the MØ response towards immune-related functions. Importantly, these differences in the DEGs show that even in the apparent absence of qualitative molecular differences in PEVs and their targeted inflammatory mediator cargo, the PEVs were able to execute differential programming of the MØs. We cannot exclude, however, the possibility of cargo differences between the PEV types e.g. in terms of non-coding large or small RNAs or metabolites that could affect MØ transcriptome and explain the observed differences.

The complexity of performing functional studies, especially regarding the dosage and a correct time window for treatment, is generally acknowledged in the EV field (Nguyen et al., 2020) and in the future, more focus should be set on these aspects. Despite these challenges and the large biological variation between the human donors for platelets and MØs, the PEVs from activated platelets clearly modulated the gene signature even in the presence of a strong polarization stimulus.

In the present study, the human lipoproteins were in-house isolated and modified by well-established methods, and the PEVs were characterized according to the MISEV guidelines (Thery et al., 2018) using contemporary EV analyses such as high-sensitivity flow cytometry dedicated for the detection of submicron particles. In the past, conventional flow cytometers have often been used to analyze patient EV samples. However, the early EV flow cytometry data may have limited utility, due to the lack of sensitivity of the used flow cytometers to detect particles smaller than 500 nm (Robert et al., 2009; Dickhout and Koenen, 2018). Furthermore, the use of polystyrene beads to gate EVs may lead to misinterpretation of the results since such gates may not detect the real (P)EV populations [reviewed in (Kuiper et al., 2021)]. This is especially critical if residual platelets are not adequately removed (Palviainen et al., 2020), since for example a side scatter gate on 400–800 nm polystyrene beads approximately detects particles in the size range of platelets (Van Der Pol et al., 2018). In this study, the removal of residual platelets was performed with particular care throughout the study and verified by a clinical platelet counter. Furthermore, a light scatter calibration (Rosetta calibration system from Exometry, The Netherlands) was used to define EV diameter gates (200–1000 nm). With the emergence of detailed guidelines for EV detection by flow cytometry including MIFlowCyt-EV (Welsh et al., 2020; Van Der Pol et al., 2022; Welsh et al., 2023), it will be beneficial to return to the analysis of PEVs from samples of atherosclerotic patients.

By demonstrating that oxLDL potentiates the formation of procoagulant and adhesive PEVs from activated platelets, and that such PEVs modify the MØ phenotype and transcriptome, the present study provides new insight into the mechanisms by which oxLDL and platelets may contribute to atherogenesis. As the atherosclerotic processes are multicellular involving also endothelial cells, neutrophils, and T lymphocytes in addition to monocytes, this study should be followed by investigations of the impact of oxLDL PEVs on these cell types. Moreover, the effect of oxLDL+TC activation on platelet/monocyte aggregates would be worth studying, as it was recently shown that the resulting EVs from this interaction were proatherogenic in vitro and similar EVs were detectable in patients suffering from carotid artery disease (Oggero et al., 2021). Finally, elucidating the spatiotemporal generation of different PEV subpopulations and their effector cargo as well as the relevance of circulating PEVs in vivo will be crucial for pinpointing the true role of PEVs in atherogenesis.

Funding

This work was supported by the Academy of Finland [grants 287089 (PRMS and MN), 330486 (PRMS and MP), 332761 (DG and AF), and 332564 (KÖ)]; Business Finland [grant EVE (PRMS and KM)]; Magnus Ehrnrooth Foundation (PRMS); Finnish Foundation for Cardiovascular Research (MN and KÖ); Swedish Research Council [grant 2020–02258 (MKM)]; Medicinska Understödsföreningen Liv och Hälsa rf (PRMS); and Novo Nordisk Foundation [grant NNF19OC0057411 (KÖ)]. The funders had no role in the design of the study, in the collection, analysis, or interpretation of the data, in the writing of the manuscript, or in the decision to publish the results.

CRediT authorship contribution statement

Katariina Maaninka: Conceptualization, Methodology, Formal analysis, Investigation, Data curation, Writing – original draft, Writing – review & editing, Visualization. **Maarit Neuvonen:** Conceptualization, Methodology, Investigation, Writing – original draft, Writing – review & editing. **Erja Kerkelä:** Methodology, Formal analysis, Investigation, Writing – review & editing, Visualization. **Kati Hyvärinen:** Methodology, Investigation, Writing – review & editing. **Mari Palviainen:** Formal analysis, Writing – review & editing. **Masood Kamali-Moghaddam:** Methodology, Investigation, Resources, Writing – review & editing. **Antonio Federico:** Software, Formal analysis, Writing – review & editing, Visualization. **Dario Greco:** Resources, Writing – review & editing. **Saara Laitinen:** Resources, Writing – review & editing. **Katariina Öörni:** Methodology, Resources, Writing – review & editing. **Pia RM Siljander:** Conceptualization, Methodology, Writing – review & editing, Supervision, Funding acquisition.

Declaration of Competing Interest

The authors declare that they have no known competing financial interests or personal relationships that could have appeared to influence the work reported in this paper.

Data availability

The transcriptomic data are available in Figshare at https://figshare.com/s/d71a9686497613251465 Additional data that support this study are available in the supplementary material.

Acknowledgements

We thank the services of University of Helsinki: EV Core in FIMM Technology Centre supported by the HiLIFE and Biocenter Finland for

performing electron microscopy work and Electron Microscopy Unit of the Institute of Biotechnology for providing the facilities. We also thank Core facility Sequencing Unit at FIMM Technology Centre supported by the University of Helsinki and Biocenter Finland, and PLA and Single Cell Facility Swedish SciLifeLab for PEA analysis. Dr. Matti Jauhianen is thanked for kindly providing HDL and the anti-ApoB monoclonal antibody for the experiments.

Appendix A. Supporting information

Supplementary data associated with this article can be found in the online version at doi:10.1016/j.ejcb.2023.151311.

References

Aatonen, M., Grönholm, M., Siljander, P.R., 2012. Platelet-derived microvesicles: multitalented participants in intercellular communication. Semin Thromb. Hemost. 38, 102–113.
Aatonen, M.T., Ohman, T., Nyman, T.A., Laitinen, S., Gronholm, M., Siljander, P.R., 2014. Isolation and characterization of platelet-derived extracellular vesicles. J. Extracell Vesicles 3.
Ardlie, N.G., Selley, M.L., Simons, L.A., 1989. Platelet activation by oxidatively modified low density lipoproteins. Atherosclerosis 76, 117–124.
Assarsson, E., Lundberg, M., Holmquist, G., Bjorkesten, J., Thorsen, S.B., Ekman, D., Eriksson, A., Rennel Dickens, E., Ohlsson, S., Edfeldt, G., Andersson, A.C., Lindstedt, P., Stenvang, J., Gullberg, M., Fredriksson, S., 2014. Homogenous 96-plex PEA immunoassay exhibiting high sensitivity, specificity, and excellent scalability. PLoS One 9, e95192.
Bäck, M., Yurdagul, A., J.R., Tabas, I., Öörni, K., Kovanen, P.T., 2019. Inflammation and its resolution in atherosclerosis: mediators and therapeutic opportunities. Nat. Rev. Cardiol. 16, 389–406.
Badimon, L., Padro, T., Arderiu, G., Vilahur, G., Borrell-Pages, M., Suades, R., 2022. Extracellular vesicles in atherothrombosis: From biomarkers and precision medicine to therapeutic targets. Immunol. Rev. 312, 6–19.
Badrnya, S., Schrottmaier, W.C., Kral, J.B., Yaiw, K.C., Volf, I., Schabbauer, G., Soderberg-Naucler, C., Assinger, A., 2014. Platelets mediate oxidized low-density lipoprotein-induced monocyte extravasation and foam cell formation. Arterioscler. Thromb. Vasc. Biol. 34, 571–580.
Baj-Krzyworzeka, M., Majka, M., Pratico, D., Ratajczak, J., Vilaire, G., Kijowski, J., Reca, R., Janowska-Wieczorek, A., Ratajczak, M.Z., 2002. Platelet-derived microparticles stimulate proliferation, survival, adhesion, and chemotaxis of hematopoietic cells. Exp. Hematol. 30, 450–459.
Barrett, T.J., 2020. Macrophages in atherosclerosis regression. Arterioscler. Thromb. Vasc. Biol. 40, 20–33.
Barrett, T.J., Schlegel, M., Zhou, F., Gorenchtein, M., Bolstorff, J., Moore, K.J., Fisher, E. A., Berger, J.S., 2019. Platelet regulation of myeloid suppressor of cytokine signaling 3 accelerates atherosclerosis. Sci. Transl. Med 11.
Berger, M., Raslan, Z., Aburima, A., Magwenzi, S., Wraith, K.S., Spurgeon, B.E.J., Hindle, M.S., Law, R., Febbraio, M., Naseem, K.M., 2020. Atherogenic lipid stress induces platelet hyperactivity through CD36-mediated hyposensitivity to prostacyclin: the role of phosphodiesterase 3A. Haematologica 105, 808–819.
Biswas, S., Zimman, A., Gao, D., Byzova, T.V., Podrez, E.A., 2017. TLR2 Plays a Key Role in Platelet Hyperreactivity and Accelerated Thrombosis Associated With Hyperlipidemia. Circ. Res 121, 951–962.
Boilard, E., 2018. Extracellular vesicles and their content in bioactive lipid mediators: more than a sack of microRNA. J. Lipid Res 59, 2037–2046.
Boilard, E., Duchez, A.C., Brisson, A., 2015. The diversity of platelet microparticles. Curr. Opin. Hematol. 22, 437–444.
Boren, J., Chapman, M.J., Krauss, R.M., Packard, C.J., Bentzon, J.F., Binder, C.J., Daemen, M.J., Demer, L.L., Hegele, R.A., Nicholls, S.J., Nordestgaard, B.G., Watts, G. F., Bruckert, E., Fazio, S., Ference, B.A., Graham, I., Horton, J.D., Landmesser, U., Laufs, U., Masana, L., Pasterkamp, G., Raal, F.J., Ray, K.K., Schunkert, H., Taskinen, M.R., VAN De Sluis, B., Wiklund, O., Tokgozoglu, L., Catapano, A.L., Ginsberg, H.N., 2020. Low-density lipoproteins cause atherosclerotic cardiovascular disease: pathophysiological, genetic, and therapeutic insights: a consensus statement from the European Atherosclerosis Society Consensus Panel. Eur. Heart J. 41, 2313–2330.
Calvo, D., Gomez-Coronado, D., Suarez, Y., Lasuncion, M.A., Vega, M.A., 1998. Human CD36 is a high affinity receptor for the native lipoproteins HDL, LDL, and VLDL. J. Lipid Res 39, 777–788.
Carvalho, A.C., Colman, R.W., Lees, R.S., 1974. Platelet function in hyperlipoproteinemia. N. Engl. J. Med 290, 434–438.
Colas, R., Sassolas, A., Guichardant, M., Cugnet-Anceau, C., Moret, M., Moulin, P., Lagarde, M., Calzada, C., 2011. LDL from obese patients with the metabolic syndrome show increased lipid peroxidation and activate platelets. Diabetologia 54, 2931–2940.
Coly, P.M., Boulanger, C.M., 2022. Role of extracellular vesicles in atherosclerosis: An update. J. Leukoc. Biol. 111, 51–62.
Connelly, M.A., Klein, S.M., Azhar, S., Abumrad, N.A., Williams, D.L., 1999. Comparison of class B scavenger receptors, CD36 and scavenger receptor BI (SR-BI), shows that both receptors mediate high density lipoprotein-cholesteryl ester selective uptake but SR-BI exhibits a unique enhancement of cholesteryl ester uptake. J. Biol. Chem. 274, 41–47.
Davi, G., Romano, M., Mezzetti, A., Procopio, A., Iacobelli, S., Antidormi, T., Bucciarelli, T., Alessandrini, P., Cuccurullo, F., Bittolo Bon, G., 1998. Increased levels of soluble P-selectin in hypercholesterolemic patients. Circulation 97, 953–957.
Davizon-Castillo, P., Mcmahon, B., Aguila, S., Bark, D., Ashworth, K., Allawzi, A., Campbell, R.A., Montenont, E., Nemkov, T., D'alessandro, A., Clendenen, N., Shih, L., Sanders, N.A., Higa, K., Cox, A., Padilla-Romo, Z., Hernandez, G., Wartchow, E., Trahan, G.D., Nozik-Grayck, E., Jones, K., Pietras, E.M., Degregori, J., Rondina, M.T., Di Paola, J., 2019. TNF-alpha-driven inflammation and mitochondrial dysfunction define the platelet hyperreactivity of aging. Blood 134, 727–740.
De Sousa, J.R., Da Costa Vasconcelos, P.F., Quaresma, J.A.S., 2019. Functional aspects, phenotypic heterogeneity, and tissue immune response of macrophages in infectious diseases. Infect. Drug Resist 12, 2589–2611.
Dean, W.L., Lee, M.J., Cummins, T.D., Schultz, D.J., Powell, D.W., 2009. Proteomic and functional characterisation of platelet microparticle size classes. Thromb. Haemost. 102, 711–718.
Dickhout, A., Koenen, R.R., 2018. Extracellular vesicles as biomarkers in cardiovascular disease; chances and risks. Front Cardiovasc Med 5, 113.
Durinck, S., Spellman, P.T., Birney, E., Huber, W., 2009. Mapping identifiers for the integration of genomic datasets with the R/Bioconductor package biomaRt. Nat. Protoc. 4, 1184–1191.
Erbel, C., Wolf, A., Lasitschka, F., Linden, F., Domschke, G., Akhavanpoor, M., Doesch, A. O., Katus, H.A., Gleissner, C.A., 2015. Prevalence of M4 macrophages within human coronary atherosclerotic plaques is associated with features of plaque instability. Int J. Cardiol. 186, 219–225.
Faria, A.V.S., Andrade, S.S., Peppelenbosch, M.P., Ferreira-Halder, C.V., Fuhler, G.M., 2020. Platelets in aging and cancer-"double-edged sword". Cancer Metastasis Rev. 39, 1205–1221.
Ference, B.A., Ginsberg, H.N., Graham, I., Ray, K.K., Packard, C.J., Bruckert, E., Hegele, R.A., Krauss, R.M., Raal, F.J., Schunkert, H., Watts, G.F., Boren, J., Fazio, S., Horton, J.D., Masana, L., Nicholls, S.J., Nordestgaard, B.G., VAN De Sluis, B., Taskinen, M.R., Tokgozoglu, L., Landmesser, U., Laufs, U., Wiklund, O., Stock, J.K., Chapman, M.J., Catapano, A.L., 2017. Low-density lipoproteins cause atherosclerotic cardiovascular disease. 1. Evidence from genetic, epidemiologic, and clinical studies. A consensus statement from the European Atherosclerosis Society Consensus Panel. Eur. Heart J. 38, 2459–2472.
Ferreira, P.M., Bozbas, E., Tannetta, S.D., Alroqaiba, N., Zhou, R., Crawley, J.T.B., Gibbins, J.M., Jones, C.I., Ahnstrom, J., Yaqoob, P., 2020. Mode of induction of platelet-derived extracellular vesicles is a critical determinant of their phenotype and function. Sci. Rep. 10, 18061.
Gasecka, A., Nieuwland, R., Siljander, P., 2019. Platelet extracellular vesicles. In: Michelson, A., Cattaneo, M., Frelinger, A., Newman, P. (Eds.), Platelets., 4 ed.,. Academic Press, pp. 401–416.
Gleissner, C.A., Shaked, I., Little, K.M., Ley, K., 2010. CXC chemokine ligand 4 induces a unique transcriptome in monocyte-derived macrophages. J. Immunol. 184, 4810–4818.
Harmon, J.T., Tandon, N.N., Hoeg, J.M., Jamieson, G.A., 1986. Thrombin binding and response in platelets from patients with dyslipoproteinemias: increased stimulus-response coupling in type II hyperlipoproteinemia. Blood 68, 498–505.
Havel, R.J., Eder, H.A., Bragdon, J.H., 1955. The distribution and chemical composition of ultracentrifugally separated lipoproteins in human serum. J. Clin. Invest 34, 1345–1353.
Hessler, J.R., Morel, D.W., Lewis, L.J., Chisolm, G.M., 1983. Lipoprotein oxidation and lipoprotein-induced cytotoxicity. Arteriosclerosis 3, 215–222.
Hulten, L.M., Ullstrom, C., Krettek, A., VAN Reyk, D., Marklund, S.L., Dahlgren, C., Wiklund, O., 2005. Human macrophages limit oxidation products in low density lipoprotein. Lipids Health Dis. 4, 6.
Hyvärinen, K., Holopainen, M., Skirdenko, V., Ruhanen, H., Lehenkari, P., Korhonen, M., Käkelä, R., Laitinen, S., Kerkelä, E., 2018. Mesenchymal Stromal Cells and Their Extracellular Vesicles Enhance the Anti-Inflammatory Phenotype of Regulatory Macrophages by Downregulating the Production of Interleukin (IL)-23 and IL-22. Front Immunol. 9, 771.
Konkoth, A., Saraswat, R., Dubrou, C., Sabatier, F., Leroyer, A.S., Lacroix, R., Duchez, A. C., Dignat-George, F., 2021. Multifaceted role of extracellular vesicles in atherosclerosis. Atherosclerosis 319, 121–131.
Korporaal, S.J., Gorter, G., Van Rijn, H.J., Akkerman, J.W., 2005. Effect of oxidation on the platelet-activating properties of low-density lipoprotein. Arterioscler. Thromb. Vasc. Biol. 25, 867–872.
Korporaal, S.J., Van Eck, M., Adelmeijer, J., Ijsseldijk, M., Out, R., Lisman, T., Lenting, P. J., Van Berkel, T.J., Akkerman, J.W., 2007. Platelet activation by oxidized low density lipoprotein is mediated by CD36 and scavenger receptor-A. Arterioscler. Thromb. Vasc. Biol. 27, 2476–2483.
Kuiper, M., Van De Nes, A., Nieuwland, R., Varga, Z., Van Der Pol, E., 2021. Reliable measurements of extracellular vesicles by clinical flow cytometry. Am. J. Reprod. Immunol. 85, e13350.
Kumar, A., Kankainen, M., Parsons, A., Kallioniemi, O., Mattila, P., Heckman, C.A., 2017. The impact of RNA sequence library construction protocols on transcriptomic profiling of leukemia. BMC Genom. 18, 629.
Kuriyama, N., Nagakane, Y., Hosomi, A., Ohara, T., Kasai, T., Harada, S., Takeda, K., Yamada, K., Ozasa, K., Tokuda, T., Watanabe, Y., Mizuno, T., Nakagawa, M., 2010. Evaluation of factors associated with elevated levels of platelet-derived microparticles in the acute phase of cerebral infarction. Clin. Appl. Thromb. Hemost. 16, 26–32.

Lara-Guzman, O.J., Gil-Izquierdo, A., Medina, S., Osorio, E., Alvarez-Quintero, R., Zuluaga, N., Oger, C., Galano, J.M., Durand, T., Munoz-Durango, K., 2018. Oxidized LDL triggers changes in oxidative stress and inflammatory biomarkers in human macrophages. Redox Biol. 15, 1–11.
Larssen, P., Wik, L., Czarnewski, P., Eldh, M., Lof, L., Ronquist, K.G., Dubois, L., Freyhult, E., Gallant, C.J., Oelrich, J., Larsson, A., Ronquist, G., Villablanca, E.J., Landegren, U., Gabrielsson, S., Kamali-Moghaddam, M., 2017. Tracing Cellular Origin of Human Exosomes Using Multiplex Proximity Extension Assays. Mol. Cell Proteom. 16, 1547.
Larsson, A., Carlsson, L., Gordh, T., Lind, A.L., Thulin, M., Kamali-Moghaddam, M., 2015. The effects of age and gender on plasma levels of 63 cytokines. J. Immunol. Methods 425, 58–61.
Lehti, S., Nguyen, S.D., Belevich, I., Vihinen, H., Heikkila, H.M., Soliymani, R., Kakela, R., Saksi, J., Jauhiainen, M., Grabowski, G.A., Kummu, O., Horkko, S., Baumann, M., Lindsberg, P.J., Jokitalo, E., Kovanen, P.T., Oorni, K., 2018. Extracellular Lipids Accumulate in Human Carotid Arteries as Distinct Three-Dimensional Structures and Have Proinflammatory Properties. Am. J. Pathol. 188, 525–538.
Levitan, I., Volkov, S., Subbaiah, P.V., 2010. Oxidized LDL: diversity, patterns of recognition, and pathophysiology. Antioxid. Redox Signal 13, 39–75.
Love, M.I., Huber, W., Anders, S., 2014. Moderated estimation of fold change and dispersion for RNA-seq data with DESeq2. Genome Biol. 15, 550.
Lukasik, M., Rozalski, M., Luzak, B., Michalak, M., Ambrosius, W., Watala, C., Kozubski, W., 2013. Enhanced platelet-derived microparticle formation is associated with carotid atherosclerosis in convalescent stroke patients. Platelets 24, 63–70.
Ma, Q., Fan, Q., Han, X., Dong, Z., Xu, J., Bai, J., Tao, W., Sun, D., Wang, C., 2021. Platelet-derived extracellular vesicles to target plaque inflammation for effective anti-atherosclerotic therapy. J. Control Release 329, 445–453.
Magwenzi, S., Woodward, C., Wraith, K.S., Aburima, A., Raslan, Z., Jones, H., Mcneil, C., Wheatcroft, S., Yuldasheva, N., Febbriao, M., Kearney, M., Naseem, K.M., 2015. Oxidized LDL activates blood platelets through CD36/NOX2-mediated inhibition of the cGMP/protein kinase G signaling cascade. Blood 125, 2693–2703.
Martinez, F.O., Gordon, S., 2014. The M1 and M2 paradigm of macrophage activation: time for reassessment. F1000Prime Rep. 6, 13.
Massberg, S., Brand, K., Gruner, S., Page, S., Muller, E., Muller, I., Bergmeier, W., Richter, T., Lorenz, M., Konrad, I., Nieswandt, B., Gawaz, M., 2002. A critical role of platelet adhesion in the initiation of atherosclerotic lesion formation. J. Exp. Med 196, 887–896.
Milioli, M., Ibanez-Vea, M., Sidoli, S., Palmisano, G., Careri, M., Larsen, M.R., 2015. Quantitative proteomics analysis of platelet-derived microparticles reveals distinct protein signatures when stimulated by different physiological agonists. J. Proteom. 121, 56–66.
Nergiz-Unal, R., Lamers, M.M., Van Kruchten, R., Luiken, J.J., Cosemans, J.M., Glatz, J. F., Kuijpers, M.J., Heemskerk, J.W., 2011. Signaling role of CD36 in platelet activation and thrombus formation on immobilized thrombospondin or oxidized low-density lipoprotein. J. Thromb. Haemost. 9, 1835–1846.
Nguyen, V.V.T., Witwer, K.W., Verhaar, M.C., Strunk, D., Van Balkom, B.W.M., 2020. Functional assays to assess the therapeutic potential of extracellular vesicles. J. Extracell Vesicles 10, e12033.
Nielsen, T.B., Nielsen, M.H., Handberg, A., 2015. In vitro Incubation of Platelets with oxLDL Does Not Induce Microvesicle Release When Measured by Sensitive Flow Cytometry. Front Cardiovasc Med 2, 37.
Oggero, S., DE Gaetano, M., Marcone, S., Fitzsimons, S., Pinto, A.L., Ikramova, D., Barry, M., Burke, D., Montero-Melendez, T., Cooper, D., Burgoyne, T., Belton, O., Norling, L.V., Brennan, E.P., Godson, C., Perretti, M., 2021. Extracellular vesicles from monocyte/platelet aggregates modulate human atherosclerotic plaque reactivity. J. Extracell Vesicles 10, 12084.
Palviainen, M., Saraswat, M., Varga, Z., Kitka, D., Neuvonen, M., Puhka, M., Joenvaara, S., Renkonen, R., Nieuwland, R., Takatalo, M., Siljander, P.R.M., 2020. Extracellular vesicles from human plasma and serum are carriers of extravesicular cargo-Implications for biomarker discovery. PLoS One 15, e0236439.
Panigrahi, S., Ma, Y., Hong, L., Gao, D., West, X.Z., Salomon, R.G., Byzova, T.V., Podrez, E.A., 2013. Engagement of platelet toll-like receptor 9 by novel endogenous ligands promotes platelet hyperreactivity and thrombosis. Circ. Res 112, 103–112.
Pienimaeki-Roemer, A., Fischer, A., Tafelmeier, M., Orso, E., Konovalova, T., Bottcher, A., Liebisch, G., Reidel, A., Schmitz, G., 2014. High-density lipoprotein 3 and apolipoprotein A-I alleviate platelet storage lesion and release of platelet extracellular vesicles. Transfusion 54, 2301–2314.
Podrez, E.A., Byzova, T.V., Febbraio, M., Salomon, R.G., Ma, Y., Valiyaveettil, M., Poliakov, E., Sun, M., Finton, P.J., Curtis, B.R., Chen, J., Zhang, R., Silverstein, R.L., Hazen, S.L., 2007. Platelet CD36 links hyperlipidemia, oxidant stress and a prothrombotic phenotype. Nat. Med 13, 1086–1095.
Puhka, M., Nordberg, M.E., Valkonen, S., Rannikko, A., Kallioniemi, O., Siljander, P., Af, Hallstrom, T.M., 2017. KeepEX, a simple dilution protocol for improving extracellular vesicle yields from urine. Eur. J. Pharm. Sci. 98, 30–39.
Puhm, F., Boilard, E., Machlus, K.R., 2021. Platelet extracellular vesicles: beyond the blood. Arterioscler. Thromb. Vasc. Biol. 41, 87–96.
Radding, C.M., Steinberg, D., 1960. Studies on the synthesis and secretion of serum lipoproteins by rat liver slices. J. Clin. Invest 39, 1560–1569.
Robert, S., Poncelet, P., Lacroix, R., Arnaud, L., Giraudo, L., Hauchard, A., Sampol, J., Dignat-George, F., 2009. Standardization of platelet-derived microparticle counting using calibrated beads and a Cytomics FC500 routine flow cytometer: a first step towards multicenter studies? J. Thromb. Haemost. 7, 190–197.
Rubic, T., Lorenz, R.L., 2006. Downregulated CD36 and oxLDL uptake and stimulated ABCA1/G1 and cholesterol efflux as anti-atherosclerotic mechanisms of interleukin-10. Cardiovasc Res 69, 527–535.
Saboor, M., Ayub, Q., Ilyas, S.Moinuddin, 2013. Platelet receptors; an instrumental of platelet physiology. Pak. J. Med Sci. 29, 891–896.
Sachais, B.S., Turrentine, T., Dawicki Mckenna, J.M., Rux, A.H., Rader, D., Kowalska, M. A., 2007. Elimination of platelet factor 4 (PF4) from platelets reduces atherosclerosis in C57Bl/6 and apoE-/- mice. Thromb. Haemost. 98, 1108–1113.
Sadallah, S., Eken, C., Martin, P.J., Schifferli, J.A., 2011. Microparticles (ectosomes) shed by stored human platelets downregulate macrophages and modify the development of dendritic cells. J. Immunol. 186, 6543–6552.
Sadallah, S., Amicarella, F., Eken, C., Iezzi, G., Schifferli, J.A., 2014. Ectosomes released by platelets induce differentiation of CD4+T cells into T regulatory cells. Thromb. Haemost. 112, 1219–1229.
Scheuerer, B., Ernst, M., Durrbaum-Landmann, I., Fleischer, J., Grage-Griebenow, E., Brandt, E., Flad, H.D., Petersen, F., 2000. The CXC-chemokine platelet factor 4 promotes monocyte survival and induces monocyte differentiation into macrophages. Blood 95, 1158–1166.
Shastri, K.M., Carvalho, A.C., Lees, R.S., 1980. Platelet function and platelet lipid composition in the dyslipoproteinemias. J. Lipid Res 21, 467–472.
Siljander, P., Lassila, R., 1999. Studies of adhesion-dependent platelet activation: distinct roles for different participating receptors can be dissociated by proteolysis of collagen. Arterioscler. Thromb. Vasc. Biol. 19, 3033–3043.
Soldano, S., Trombetta, A.C., Contini, P., Tomatis, V., Ruaro, B., Brizzolara, R., Montagna, P., Sulli, A., Paolino, S., Pizzorni, C., Smith, V., Cutolo, M., 2018. Increase in circulating cells coexpressing M1 and M2 macrophage surface markers in patients with systemic sclerosis. Ann. Rheum. Dis. 77, 1842–1845.
Steinberg, D., Witztum, J.L., 2010. Oxidized low-density lipoprotein and atherosclerosis. Arterioscler. Thromb. Vasc. Biol. 30, 2311–2316.
Suades, R., Padro, T., Alonso, R., Mata, P., Badimon, L., 2015. High levels of TSP1+/CD142+ platelet-derived microparticles characterise young patients with high cardiovascular risk and subclinical atherosclerosis. Thromb. Haemost. 114, 1310–1321.
Suades, R., Padro, T., Crespo, J., Sionis, A., Alonso, R., Mata, P., Badimon, L., 2019. Liquid Biopsy of Extracellular Microvesicles Predicts Future Major Ischemic Events in Genetically Characterized Familial Hypercholesterolemia Patients. Arterioscler. Thromb. Vasc. Biol. 39, 1172–1181.
Suades, R., Padro, T., Vilahur, G., Badimon, L., 2022. Platelet-released extracellular vesicles: the effects of thrombin activation. Cell Mol. Life Sci. 79, 190.
Takahashi, Y., Chiba, H., Matsuno, K., Akita, H., Hui, S.P., Nagasaka, H., Nakamura, H., Kobayashi, K., Tandon, N.N., Jamieson, G.A., 1996. Native lipoproteins inhibit platelet activation induced by oxidized lipoproteins. Biochem Biophys. Res Commun. 222, 453–459.
Tan, K.T., Tayebjee, M.H., Lim, H.S., Lip, G.Y., 2005. Clinically apparent atherosclerotic disease in diabetes is associated with an increase in platelet microparticle levels. Diabet. Med 22, 1657–1662.
Tarazona, S., Furio-Tari, P., Turra, D., Pietro, A.D., Nueda, M.J., Ferrer, A., Conesa, A., 2015. Data quality aware analysis of differential expression in RNA-seq with NOISeq R/Bioc package. Nucleic Acids Res 43, e140.
Taus, F., Meneguzzi, A., Castelli, M., Minuz, P., 2019. Platelet-Derived Extracellular Vesicles as Target of Antiplatelet Agents. What Is the Evidence? Front Pharm. 10, 1256.
Thery, C., Witwer, K.W., Aikawa, E., Alcaraz, M.J., Anderson, J.D., Andriantsitohaina, R., Antoniou, A., Arab, T., Archer, F., Atkin-Smith, G.K., Ayre, D.C., Bach, J.M., Bachurski, D., Baharvand, H., Balaj, L., Baldacchino, S., Bauer, N.N., Baxter, A.A., Bebawy, M., Beckham, C., Bedina Zavec, A., Benmoussa, A., Berardi, A.C., Bergese, P., Bielska, E., Blenkiron, C., Bobis-Wozowicz, S., Boilard, E., Boireau, W., Bongiovanni, A., Borras, F.E., Bosch, S., Boulanger, C.M., Breakefield, X., Breglio, A. M., Brennan, M.A., Brigstock, D.R., Brisson, A., Broekman, M.L., Bromberg, J.F., Bryl-Gorecka, P., Buch, S., Buck, A.H., Burger, D., Busatto, S., Buschmann, D., Bussolati, B., Buzas, E.I., Byrd, J.B., Camussi, G., Carter, D.R., Caruso, S., Chamley, L. W., Chang, Y.T., Chen, C., Chen, S., Cheng, L., Chin, A.R., Clayton, A., Clerici, S.P., Cocks, A., Cocucci, E., Coffey, R.J., Cordeiro-Da-Silva, A., Couch, Y., Coumans, F.A., Coyle, B., Crescitelli, R., Criado, M.F., D'souza-Schorey, C., Das, S., Datta Chaudhuri, A., De Candia, P., De Santana, E.F., De Wever, O., Del Portillo, H.A., Demaret, T., Deville, S., Devitt, A., Dhondt, B., Di Vizio, D., Dieterich, L.C., Dolo, V., Dominguez Rubio, A.P., Dominici, M., Dourado, M.R., Driedonks, T.A., Duarte, F.V., Duncan, H.M., Eichenberger, R.M., Ekstrom, K., El Andaloussi, S., Elie-Caille, C., Erdbrugger, U., Falcon-Perez, J.M., Fatima, F., Fish, J.E., Flores-Bellver, M., Forsonits, A., Frelet-Barrand, A., et al., 2018. Minimal information for studies of extracellular vesicles 2018 (MISEV2018): a position statement of the International Society for Extracellular Vesicles and update of the MISEV2014 guidelines. J. Extracell Vesicles 7, 1535750.
Trombetta, A.C., Soldano, S., Contini, P., Tomatis, V., Ruaro, B., Paolino, S., Brizzolara, R., Montagna, P., Sulli, A., Pizzorni, C., Smith, V., Cutolo, M., 2018. A circulating cell population showing both M1 and M2 monocyte/macrophage surface markers characterizes systemic sclerosis patients with lung involvement. Respir. Res 19, 186.
Trpkovic, A., Resanovic, I., Stanimirovic, J., Radak, D., Mousa, S.A., Cenic-Milosevic, D., Jevremovic, D., Isenovic, E.R., 2015. Oxidized low-density lipoprotein as a biomarker of cardiovascular diseases. Crit. Rev. Clin. Lab Sci. 52, 70–85.
Valkonen, S., Holopainen, M., Colas, R.A., Impola, U., Dalli, J., Kakela, R., Siljander, P.R., Laitinen, S., 2019. Lipid mediators in platelet concentrate and extracellular vesicles: Molecular mechanisms from membrane glycerophospholipids to bioactive molecules. Biochim Biophys. Acta Mol. Cell Biol. Lipids 1864, 1168–1182.
Van Der Meijden, P.E.J., Heemskerk, J.W.M., 2019. Platelet biology and functions: new concepts and clinical perspectives. Nat. Rev. Cardiol. 16, 166–179.

Van Der Pol, E., Sturk, A., Van Leeuwen, T., Nieuwland, R., Coumans, F., Group, I.-S.-V. W., 2018. Standardization of extracellular vesicle measurements by flow cytometry through vesicle diameter approximation. J. Thromb. Haemost. 16, 1236–1245.

Van Der Pol, E., Welsh, J.A., Nieuwland, R., 2022. Minimum information to report about a flow cytometry experiment on extracellular vesicles: Communication from the ISTH SSC subcommittee on vascular biology. J. Thromb. Haemost. 20, 245–251.

Wang, H., Wang, Z.H., Kong, J., Yang, M.Y., Jiang, G.H., Wang, X.P., Zhong, M., Zhang, Y., Deng, J.T., Zhang, W., 2012. Oxidized low-density lipoprotein-dependent platelet-derived microvesicles trigger procoagulant effects and amplify oxidative stress. Mol. Med 18, 159–166.

Welsh, J.A., Van Der Pol, E., Arkesteijn, G.J.A., Bremer, M., Brisson, A., Coumans, F., Dignat-George, F., Duggan, E., Ghiran, I., Giebel, B., Gorgens, A., Hendrix, A., Lacroix, R., Lannigan, J., Libregts, S., Lozano-Andres, E., Morales-Kastresana, A., Robert, S., De Rond, L., Tertel, T., Tigges, J., De Wever, O., Yan, X., Nieuwland, R., Wauben, M.H.M., Nolan, J.P., Jones, J.C., 2020. MIFlowCyt-EV: a framework for standardized reporting of extracellular vesicle flow cytometry experiments. J. Extracell Vesicles 9, 1713526.

Weidtmann, A., Scheithe, R., Hrboticky, N., Pietsch, A., Lorenz, R., Siess, W., 1995. Mildly oxidized LDL induces platelet aggregation through activation of phospholipase A2. Arterioscler Thromb Vasc Biol 15 (8), 1131–1138. https://doi.org/10.1161/01.atv.15.8.1131.

Welsh, J.A., Arkesteijn, G.J.A., Bremer, M., Cimorelli, M., Dignat-George, F., Giebel, B., Gorgens, A., Hendrix, A., Kuiper, M., Lacroix, R., Lannigan, J., Van Leeuwen, T.G., Lozano-Andres, E., Rao, S., Robert, S., De Rond, L., Tang, V.A., Tertel, T., Yan, X., Wauben, M.H.M., Nolan, J.P., Jones, J.C., Nieuwland, R., Van Der Pol, E., 2023. A compendium of single extracellular vesicle flow cytometry. J. Extracell Vesicles 12, e12299.

Yang, M., Cooley, B.C., Li, W., Chen, Y., Vasquez-Vivar, J., Scoggins, N.O., Cameron, S.J., Morrell, C.N., Silverstein, R.L., 2017. Platelet CD36 promotes thrombosis by activating redox sensor ERK5 in hyperlipidemic conditions. Blood 129, 2917–2927.

Yang, M., Kholmukhamedov, A., Schulte, M.L., Cooley, B.C., Scoggins, N.O., Wood, J.P., Cameron, S.J., Morrell, C.N., Jobe, S.M., Silverstein, R.L., 2018. Platelet CD36 signaling through ERK5 promotes caspase-dependent procoagulant activity and fibrin deposition in vivo. Blood Adv. 2, 2848–2861.

Yla-Herttuala, S., Palinski, W., Rosenfeld, M.E., Parthasarathy, S., Carew, T.E., Butler, S., Witztum, J.L., Steinberg, D., 1989. Evidence for the presence of oxidatively modified low density lipoprotein in atherosclerotic lesions of rabbit and man. J. Clin. Invest 84, 1086–1095.

Yla-Herttuala, S., Palinski, W., Rosenfeld, M.E., Steinberg, D., Witztum, J.L., 1990. Lipoproteins in normal and atherosclerotic aorta. Eur. Heart J. 11 (Suppl E), 88–99.

Yu, G., Wang, L.G., Han, Y., He, Q.Y., 2012. clusterProfiler: an R package for comparing biological themes among gene clusters. OMICS 16, 284–287.

Zaldivia, M.T.K., Mcfadyen, J.D., Lim, B., Wang, X., Peter, K., 2017. Platelet-derived microvesicles in cardiovascular diseases. Front Cardiovasc Med 4, 74.

Zhang, X., Mcgeoch, S.C., Johnstone, A.M., Holtrop, G., Sneddon, A.A., Macrury, S.M., Megson, I.L., Pearson, D.W., Abraham, P., De Roos, B., Lobley, G.E., O'kennedy, N., 2014. Platelet-derived microparticle count and surface molecule expression differ between subjects with and without type 2 diabetes, independently of obesity status. J. Thromb. Thrombolysis 37, 455–463.